SlREM1 Triggers Cell Death by Activating an Oxidative Burst and Other Regulators[1]

Jianghua Cai,[a,b,2] Tong Chen,[a,2] Ying Wang,[a,b] Guozheng Qin,[a,b] and Shiping Tian[a,b,3,4]

[a]Key Laboratory of Plant Resources, Institute of Botany, Innovative Academy of Seed Design, Chinese Academy of Sciences, Beijing 100093, China

[b]University of Chinese Academy of Sciences, Yuquanlu, Beijing 100049, China

ORCID IDs: 0000-0002-2456-7170 (T.C.); 0000-0003-3046-1177 (G.Q.); 0000-0003-1837-7298 (S.T.).

Programmed cell death (PCD), a highly regulated feature of the plant immune response, involves multiple molecular players. Remorins (REMs) are plant-specific proteins with varied biological functions, but their function in PCD and plant defense remains largely unknown. Here, we report a role for remorin in disease resistance, immune response, and PCD regulation. Overexpression of tomato (*Solanum lycopersicum*) *REMORIN1* (*SlREM1*) increased susceptibility of tomato to the necrotrophic fungus *Botrytis cinerea* and heterologous expression of this gene triggered cell death in *Nicotiana benthamiana* leaves. Further investigation indicated that amino acids 173 to 187 and phosphorylation of SlREM1 played key roles in SlREM1-triggered cell death. Intriguingly, multiple tomato REMs induced cell death in *N. benthamiana* leaves. Yeast two-hybrid, split luciferase complementation, and coimmunoprecipitation assays all demonstrated that remorin proteins could form homo- and heterocomplexes. Using isobaric tags for relative and absolute quantitative proteomics, we identified that some proteins related to cell death regulation, as well as *N. benthamiana* RESPIRATORY BURST OXIDASE HOMOLOG B (which is essential for reactive oxygen species production), were notably upregulated in *SlREM1*-expressing leaves. Heterologous expression of *SlREM1* increased reactive oxygen species accumulation and triggered other cell death regulators. Our findings indicate that SlREM1 is a positive regulator of plant cell death and provide clues for understanding the PCD molecular regulatory network in plants.

Programmed cell death (PCD) serves as a fundamental biological process that is a naturally occurring suicide of cells (Lam, 2004; Fuchs and Steller, 2011). PCD in plants shows morphological and biochemical traits similar to animal apoptosis, but several characteristics differ between these two forms of PCD (Kaneda et al., 2009). Current knowledge indicates that plant PCD is closely associated with a wide variety of biological processes, including cell differentiation (Beers, 1997), aleurone layer formation (Beligni et al., 2002), tapetum degradation (Phan et al., 2011), leaf resistance (Yen and Yang, 1998), fruit resistance (Qu et al., 2009), pathogen invasion (Coll et al., 2011), and abiotic stresses (Gechev et al., 2006). Plant PCD is a complex genetically programmed mechanism, which is regulated by many factors. Reactive oxygen species (ROS) have been proven to play a vital role in the regulation of plant cell death (van Breusegem and Dat, 2006), senescence (Qin et al., 2009), and resistance response (Tian et al., 2013). Higher ROS levels attack cellular constituents and trigger cell death, whereas lower ROS levels function as a signaling compound (van Breusegem and Dat, 2006). In plants, ROS can be generated at different compartments, including the plasma membrane (PM), peroxisomes, chloroplasts, and mitochondria (Qin et al., 2009; Xie et al., 2014). ROS generated by Respiratory Burst Oxidase Homolog (RBOH) proteins have an important function in cell death, especially in hypersensitive response (HR), which is a type of PCD induced by pathogens (Lam et al., 2001; Suzuki et al., 2011). Suppression of *Nicotiana benthamiana RESPIRATORY BURST OXIDASE HOMOLOG* (*NbRBOH*) genes resulted in a reduction and delay of HR cell death caused by the protein elicitor INF1 (Yoshioka et al., 2003). Likewise, inhibition of *Oryza sativa RBOHA* expression dramatically reduced HR (Yoshie et al., 2005). Recent research indicated that SPL11 cell-death suppressor2 could induce PCD through interaction with OsRLCK118/176, which positively regulate immunity by phosphorylating the OsRBOHBs to stimulate ROS production (Fan et al., 2018).

The identification of novel cell death regulators has promoted substantial progress to deeply understand the molecular regulatory network of plant PCD. MAPK

[1]This study was supported by the National Natural Science Foundation of China (grant nos. 31930086, 31530057, and 31672210).

[2]These authors contributed equally to the article.

[3]Author for contact: tsp@ibcas.ac.cn.

[4]Senior author.

The author responsible for distribution of materials integral to the findings presented in this article in accordance with the policy described in the Instructions for Authors (www.plantphysiol.org) is: Shiping Tian (tsp@ibcas.ac.cn).

S.T. conceived the research plans; S.T. and G.Q. supervised the experiments; J.C. and T.C. performed the experiments; Y.W. provided technical assistance; J.C., T.C., and S.T. analyzed data; J.C. and S.T. wrote the article.

www.plantphysiol.org/cgi/doi/10.1104/pp.20.00120

cascade has a crucial role in the regulation of plant PCD. Overexpression of some components of MAPK cascade—*LeMAPKKKα*, *NbMEK1*, *NtMEK2*, *NtSIPK*, *NtWIPK*, and *NbNTF4*—could trigger cell death (Meng and Zhang, 2013). Transcription factors, including WRKY, NAC, ERF, LSD, HB, bHLH, and so on, have been proved to play important roles in the regulation of plant PCD, because they function as positive or negative regulators through controlling the expression of cell death inducers (Huysmans et al., 2017). Some proteases such as metacaspases, vacuolar processing enzyme, phytaspase, papain-like protease, etc. have been demonstrated to participate in regulation and execution of cell death via processing or degradation of proteins involved in cell death (Zamyatnin, 2015). Additional proteins identified as cell death regulators in plant include type-2 histone deacetylase NtHD2a and NtHD2b (Bourque et al., 2011), enoyl-acyl carrier protein reductase AtMOD1 (Wu et al., 2015), E3 ubiquitin ligase EBR1 (You et al., 2016), pathogenesis-related protein 4b CaPR4b (Hwang et al., 2014a), Cys/His-rich DC1 domain protein CaDC1 (Hwang et al., 2014b), abscisic acid-responsive1 (Choi and Hwang, 2011), RNA binding protein CaRBP1 (Lee et al., 2012), type III *Dna*J domain-containing HSP40 (Liu and Whitham, 2013), extracellular xyloglucan-specific endo-b-1,4-glucanase inhibitor protein CaXEGIP1 (Choi et al., 2013b), and cyclic nucleotide-gated ion channels AtCNGC11/12 (Urquhart et al., 2007). Nevertheless, regulators of plant PCD and their mechanisms still need to be further explored.

Remorin (REM) belongs to a plant-specific multigenic family of proteins that are present in all land plants, and widely recognized as general PM markers (Raffaele et al., 2007). Current understanding indicates that remorins display a variety of functions in plant growth, development, and signal transduction (Raffaele et al., 2007; Gui et al., 2014, 2016). In recent work, we found that overexpression of *SlREM1* in tomato (*Solanum lycopersicum*) stimulates tomato fruit ripening via mediating the expression of the genes in ethylene and lycopene biosynthesis (Cai et al., 2018). Moreover, REMs also play vital roles in plant-microbe interaction. High constitutive levels of *SlREM1.3* significantly inhibited the spread of the *Potato Virus X* through interacting with TRIPLE GENE BLOCK protein1 of *Potato Virus X* (Raffaele et al., 2009). SYMREM1 could regulate bacterial infection during nodulation *via* interaction with symbiotic receptors (Lefebvre et al., 2010). Overexpression of *SlREM1.3* in *N. benthamiana* and tomato enhanced susceptibility to *Phytophthora infestans* (Bozkurt et al., 2014). NbREM1 and OsREM1.4 could serve as negative regulators of cell-to-cell movement in *rice stripe virus* (Fu et al., 2018).

Even though some functions of REMs have been documented, in this study we report the previously unknown function of REM that serves as a positive regulator of cell death. We find that overexpression of *SlREM1* increases the susceptibility of tomato leaves to pathogenic fungal *Botrytis cinerea*, and triggers cell death in *N. benthamiana* leaves. Then, we demonstrate that SlREM1 regulates resistant response and cell death via stimulation of ROS bursts, and upregulating cell death regulators. Moreover, we demonstrate the importance of 173 to 187 amino acids and phosphorylation of SlREM1 in plant cell death. These findings not only prove that SlREM1 plays a vital role in cell death induction and disease response, but also enriches the understanding of the regulatory network of plant cell death.

RESULTS

Overexpression of *SlREM1* Enhances the Susceptibility of Tomato Leaves to *B. cinerea*, and Heterologous Expression of this Gene Triggers Cell Death in *N. benthamiana* Leaves

As previously reported, remorins play important roles in the responses to biotic stresses (Raffaele et al., 2009; Bozkurt et al., 2014). To evaluate whether SlREM1 is involved in the responses to *B. cinerea*, a necrotrophic fungus leading to massive economic losses (Li et al., 2018) and widely used as a model for plant–fungal interaction research (Zhang et al., 2014b), transgenic tomato leaves overexpressing *3×Flag-SlREM1* and suppressing *SlREM1* (*RNAi*:*SlREM1*; Supplemental Fig. S1) were inoculated with *B. cinerea* spores. A significant increase in lesion diameter was observed in *35S*:*3×Flag-SlREM1* tomato leaves compared to the wild type, whereas there was no difference between *RNAi*:*SlREM1* leaves and wild type (Fig. 1, A and B). These results indicate that overexpression of *SlREM1* enhances the susceptibility of tomato leaves to *B. cinerea*.

To further reveal the function of SlREM1 during *B. cinerea* invasion, *Agrobacterium*-mediated transient expression was performed to express *3×Flag-SlREM1* in *N. benthamiana* leaves. Surprisingly, 5 d after agroinfiltration, the infiltrated leaf areas transiently expressing *3×Flag-SlREM1* exhibited severe necrotic cell death symptoms, whereas no cell death symptom was observed in the leaves transiently expressing *3×Flag* (Fig. 1C). Immunoblot analysis with anti-Flag antibody showed that the 3×Flag-SlREM1 protein was properly expressed in infiltrated *N. benthamiana* leaves (Fig. 1D). Trypan blue staining also showed that the leaf area transiently expressing *3×Flag-SlREM1* was stained much darker compared with that transiently expressing *3×Flag* (Fig. 1E). Coincidentally, cell electrolyte leakage from leaf areas infiltrated with a *Agrobacterium* strain carrying *3×Flag-SlREM1* was also significantly higher than that from control (Fig. 1F). To further confirm the phenotype of cell death induced by SlREM1, GFP-tagged SlREM1 (GFP-SlREM1) was also transiently expressed in *N. benthamiana* leaves. Similar to *3×Flag-SlREM1*, *GFP-SlREM1*-overexpressing leaves also displayed severe cell death symptoms compared to the leaves overexpressing *GFP* (Supplemental Fig. S2, A and B). Taken together, these results indicate that transient overexpression of *SlREM1* triggers cell death in *N. benthamiana* leaves.

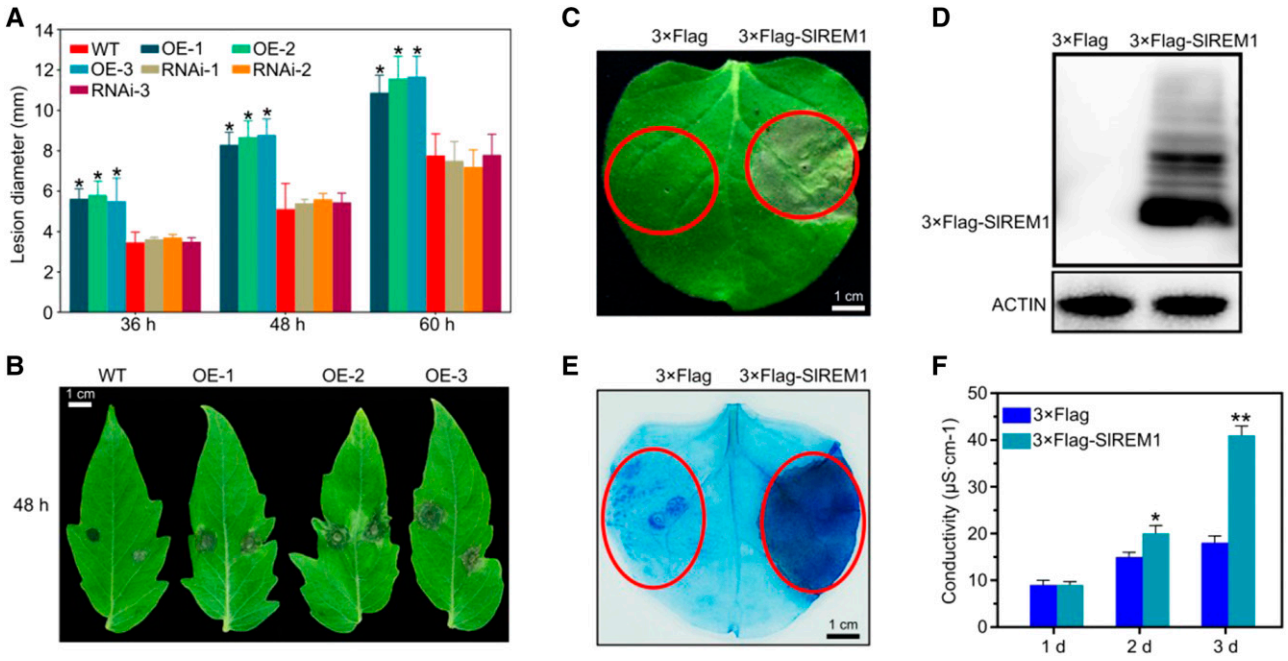

Figure 1. Overexpression of *SlREM1* decreases the resistance of tomato leaves to *B. cinerea* and induces cell death in *N. benthamiana* leaves. A, Lesion development on wild-type (WT) and *SlREM1* transgenic tomato leaves infected by *B. cinerea* (overexpression lines: OE-1, OE-2, and OE-3; RNAi lines: RNAi-1, RNAi-2, and RNAi-3). Data represent means from 24 leaves and the error bars are SD. Asterisks indicate significant differences compared with wild-type plants using ANOVA with a post hoc Tukey's Honestly Significant Difference test ($P < 0.05$). B, Disease symptoms at 48 h after inoculation with *B. cinerea* on wild-type and *SlREM1*-overexpressing (OE-1, OE-2, and OE-3) tomato leaves. The leaves were digitally extracted for comparison. C, Heterologous expression of *3×Flag-SlREM1* in *N. benthamiana* leaves triggers cell death. *N. benthamiana* leaves were infiltrated with *A. tumefaciens* strain carrying *3×Flag-SlREM1*. Cell death symptoms were photographed at 6 dpi. The red circles indicate the infiltration areas. D, Immunoblot analysis for transiently expressed *3×Flag-SlREM1* in *N. benthamiana* leaves at 2 dpi. Total proteins were isolated from *N. benthamiana* leaves transiently expressing *3×Flag-SlREM1* and *3×Flag*, respectively, followed by immunoblotting using anti-Flag antibody. ACTIN protein level was used as a loading control. E, *N. benthamiana* leaves transiently expressing *3×Flag* and *3×Flag-SlREM1* were stained using trypan blue at 5 dpi. Red circles indicate the infiltration areas. F, Determination of electrolyte leakage from leaf areas transiently expressing *3×Flag* and *3×Flag-SlREM1*. Data are means and SD of three independent biological replicates. Asterisks indicate significant differences compared with leaves expressing 3×Flag using ANOVA with a post hoc Tukey's Honestly Significant Difference test (*$P < 0.05$ and **$P < 0.01$).

Functional Domain Analysis of SlREM1

SlREM1 was proved to be exclusively localized at the PM by protoplast, colocalization, and immunoblot analysis in our previous study (Cai et al., 2018). SlREM1 protein was composed of 197 amino acids with a N-terminal region (remorin N, amino acids 25–83, pfam 03766) and a conserved C-terminal domain (remorin C, amino acids 87–192, pfam 03763). To identify which domains in SlREM1 are required for cell death induction and PM localization, colocalization analysis was performed. A series of GFP-tagged SlREM1 truncates were generated: the full-length–lacking C-terminal 35 amino acids ($SlREM1^{1–163}$), the N-terminal region ($SlREM1^{1–83}$), the C-terminal region lacking C-terminal 35 amino acids ($SlREM1^{84–163}$), the C-terminal 35 amino acids alone ($SlREM1^{CA35}$), and the C-terminal region ($SlREM1^{84–197}$), and transiently coexpressed with PM marker protein mCherry-H^+-ATPase in *N. benthamiana* leaves by agro-infiltration (Fig. 2A). The green fluorescence from SlREM1, $SlREM1^{84–197}$, and $SlREM1^{CA35}$ proteins fully colocalized with the red fluorescence from mCherry-H^+-ATPase in PM, whereas the green fluorescence from $SlREM1^{1–83}$, $SlREM1^{84–163}$, and $SlREM1^{1–163}$ proteins did not fully merge with the red fluorescence and could be detected in cytoplasm and nucleus (Fig. 2B; Supplemental Fig. S3), indicating that C-terminal 35-amino acids are necessary for PM localization of SlREM1. In addition, cell death phenotypes were also examined at 6-d post infiltration (dpi). As a consequence, only SlREM1 and $SlREM1^{84–197}$ could induce cell death (Fig. 2B). Trypan blue staining was performed to confirm the cell death symptoms (Supplemental Fig. S4).

To further identify the functional domain of SlREM1, additional truncations were generated: $SlREM1^{1–172}$ and $SlREM1^{1–187}$ (Fig. 2A). Five days after agro-infiltration, the leaves transiently expressing *GFP-SlREM1*$^{1–187}$ displayed cell death symptoms, which were not detected in the leaves transiently expressing *GFP-SlREM1*$^{1–172}$ (Fig. 2B). Subsequently, the 15 amino acids were substituted by Ala or deleted to generate $SlREM1^{1–187mu}$, $SlREM1^{1–197(15mu)}$, and $SlREM1^{1–197(15Del)}$ (Fig. 2A), respectively. GFP-tagged $SlREM1^{1–187mu}$, $SlREM1^{1–197(15mu)}$, and $SlREM1^{1–197(15Del)}$

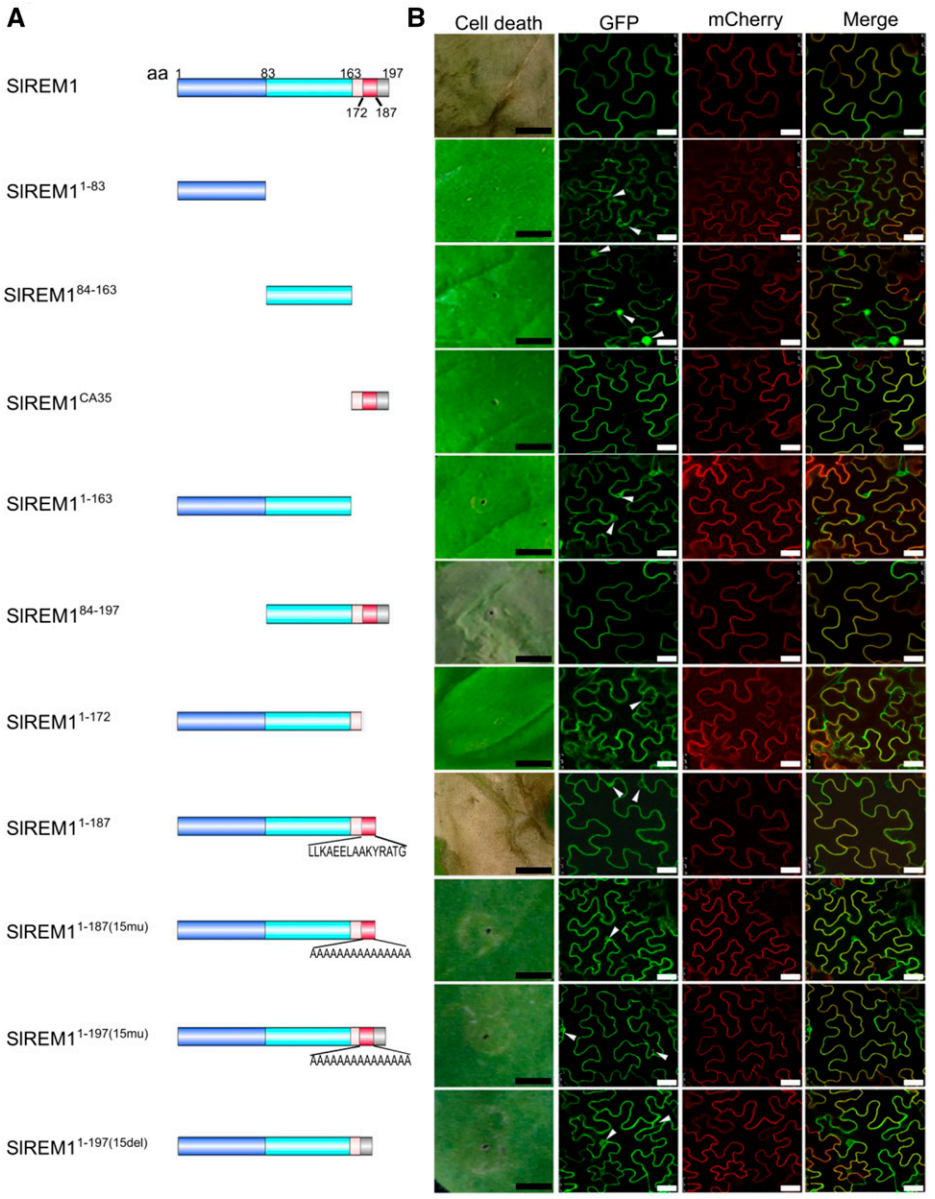

Figure 2. Functional domain analysis for SlREM1 in *N. benthamiana* leaves. A, Schematic illustration for the GFP-tagged SlREM1 truncates used in cell death and protein localization analysis.. Light blue, light aquamarine, light red, red, and gray colors represent amino acids 1 to 83, 83 to 186, 163 to 172, 172 to 187, and 187 to 197, respectively. 15mu, amino acids mutated to A(15); 15del, amino acids are deleted; aa, amino acids. B, Development of cell death phenotype and subcellular localization of various SlREM1 truncates. GFP-tagged SlREM1 truncates were transiently expressed in *N. benthamiana* leaves by agro-infiltration. Cell death symptoms were photographed at 6 dpi. For subcellular localization analysis, GFP-tagged SlREM1 (GFP) truncates were coexpressed with PM marker mCherry-H^+-ATPase (mCherry) and observed at 2 dpi. Scale bars = 0.5 cm (black) and 25 μm (white). Arrowheads indicate nuclei and cytoplasm.

were transiently expressed in *N. benthamiana* leaves, but showed no cell death phenotype in the infiltrated area (Fig. 2B; Supplemental Fig. S4). SlREM1$^{1–172}$, SlREM1$^{1–187mu}$, SlREM1$^{1–197(15mu)}$, and SlREM1$^{1–197(15Del)}$ exhibited cytoplasmic localization (Fig. 2B). These results indicate that amino acids 173 to 187 are essential for SlREM1 cell death induction as the last few amino acids were dispensable in *N. benthamiana* leaves.

Multiple Remorin Proteins in Subgroup I Are Involved in Cell Death Induction in *N. benthamiana* Leaves

To systematically study the function of remorin proteins, genes encoding remorin proteins were firstly identified from the tomato genome. Remorin proteins from Arabidopsis (*Arabidopsis thaliana*) were used as queries to search against the protein database of *S. lycopersicum* (ITAG release 3.2, Tomato Genome proteins, https://solgenomics.net/tools/blast/) to retrieve all putative remorin paralogs in tomato. Finally, a total of 19 remorin proteins were identified and listed in Supplemental Table S1. To better understand the evolutionary relationship among SlREM proteins, an unrooted neighbor-joining phylogenetic tree based on protein sequences was constructed for tomato, *N. benthamiana*, Arabidopsis, and *O. sativa*, showing that the SlREM proteins were divided into six subgroups named SlREM1 to SlREM6.4 (Supplemental Table S1). Among them, seven SlREM proteins were clustered into subgroup I and displayed the highest homology to SlREM1, whereas the other 12 SlREM proteins were allocated into five different subgroups (Fig. 3A).

To evaluate whether other SlREMs could also trigger cell death, the remorin proteins from subgroup I were

selected and transiently overexpressed in *N. benthamiana* leaves. After 5 d, trypan blue staining showed that symptoms of cell death could be also observed in the areas that infiltrated with *Agrobacterium* strains carrying *3×HA-SlREM1.4*, *3×HA-SlREM1.5*, *3×HA-SlREM1.6*, and *3×HA-SlREM1.7*, whereas no change was detected in the areas infiltrated with *3×HA-SlREM1.2* and *3×HA-SlREM1.3* (Fig. 3B). These results suggest that multiple remorin proteins in subgroup I could induce cell death in *N. benthamiana* leaves.

Remorin Proteins Can Form Homo- and Heterocomplexes

As mentioned above, multiple SlREMs could trigger cell death in *N. benthamiana* leaves, and we were curious to check whether SlREM proteins may form complexes. To test this hypothesis, yeast two hybrid (Y2H) assays were performed. As shown in Figure 4A, the yeast cells harboring SlREM1 and SlREM1, SlREM1.4, SlREM1.5, SlREM1.6, and SlREM1.7 normally grew on SD/-Leu-Trp-His-Ade agar medium and turned blue, but the yeast cells harboring SlREM1 and SlREM1.2 could not grow on SD/-Leu-Trp-His-Ade agar medium, indicating physical interaction of SlREM1 with SlREM1, SlREM1.4, SlREM1.5, SlREM1.6, and SlREM1.7. To further confirm the interaction between remorin proteins, split luciferase complementation imaging assays (LCI) were performed and SlREM1.4 and SlREM1.6 were chosen for further confirmation. *Agrobacterium tumefaciens* strains carrying Cluc-SlREM1 and SlREM1.4-Nluc and SlREM1.6-Nluc vectors were mixed and infiltrated into *N. benthamiana* leaves. Two days after infiltration, a strong luciferase signal could be detected in the leaves cotransformed with Cluc-SlREM1 and SlREM1.4-Nluc and SlREM1.6-Nluc, whereas no signal was detected in the combination of Cluc-SlREM1 with Nluc and Cluc with SlREM1.4-Nluc and SlREM1.6-Nluc (Fig. 4, B and C). Additionally, coimmunoprecipitation was conducted to confirm the interaction by coexpressing SlREM1 with 3×HA-SlREM1.4 and 3×HA-SlREM1.6 in *N. benthamiana* leaves. Anti-SlREM1 antibody and preimmune serum IgG were used for immunoprecipitation and the eluted proteins were immunoblotted using anti-HA antibody and anti-SlREM1. As shown in Figure 4, D and E, SlREM1.4 and SlREM1.6 could be specifically coprecipitated with SlREM1 by anti-SlREM1 antibody, but not by the preimmune serum. These results suggest that remorin proteins could form homo- or heterocomplexes.

To identify the core domain of SlREM1 involved in protein interaction, Y2H was performed. As shown in Figure 4F, SlREM1 and $SlREM1^{84–197}$ interacted with SlREM1.4, whereas $SlREM1^{1–163}$, $SlREM1^{1–83}$, $SlREM1^{CA35}$, and $SlREM1^{84–163}$ showed no interactions. Subsequently, LCI assays were performed to confirm the interaction. Strong luciferase signal could be detected after coexpression of Cluc-$SlREM1^{84–197}$ with SlREM1.4-Nluc in the infiltration area (Fig. 4G), whereas no luciferase signal was detected in the combination of Cluc-$SlREM1^{84–163}$ with SlREM1.4-Nluc (Supplemental Fig. S5). These results indicate that the C-terminal 35 amino acids are required but not sufficient for the hetero- and homocomplexes formation.

Quantitative Proteome Analysis Identifies Differentially Expressed Proteins in *N. benthamiana* Leaves Transiently Expressing *3×Flag-SlREM1*

To further dissect the molecular mechanism of SlREM1-induced cell death, a quantitative proteomic analysis based on isobaric tags for relative and absolute

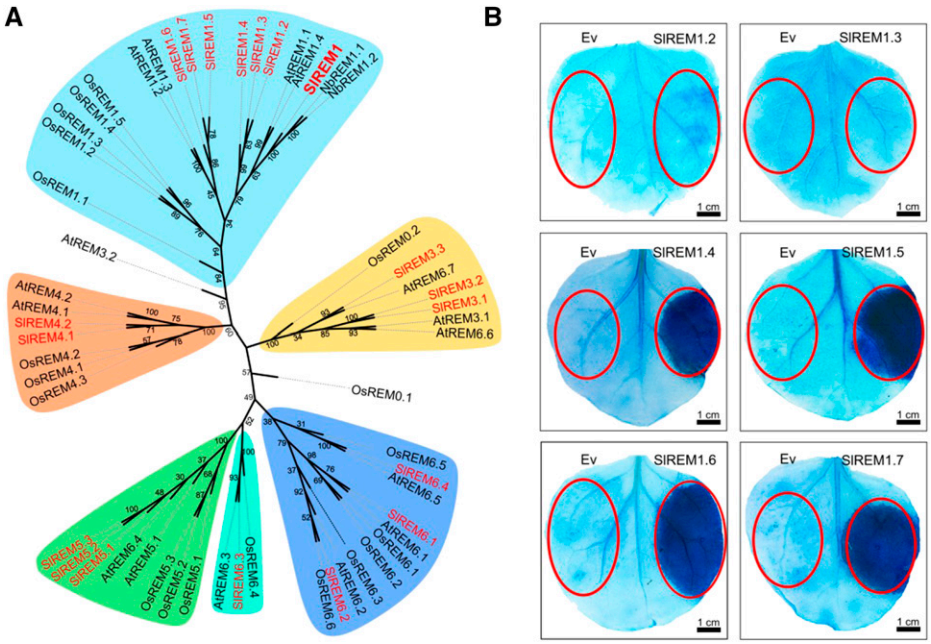

Figure 3. Multiple members in remorin family are involved in cell death induction in *N. benthamiana* leaves. A, Neighbor-joining phylogenetic analysis of remorin proteins in *S. lycopersicum*, Arabidopsis, *N. benthamiana*, and *O. sativa*. MEGA Version X was used to construct the phylogenetic tree. Bootstrap values (1,000 replicates) are shown for each branch. Tomato proteins are indicated in red. Different colors were used to highlight different groups (Groups 1–6). B, *N. benthamiana* leaves transiently expressing SlREM1.2 to S1REM1.7 were stained with trypan blue at 5 dpi. Red circles indicate the infiltration areas.

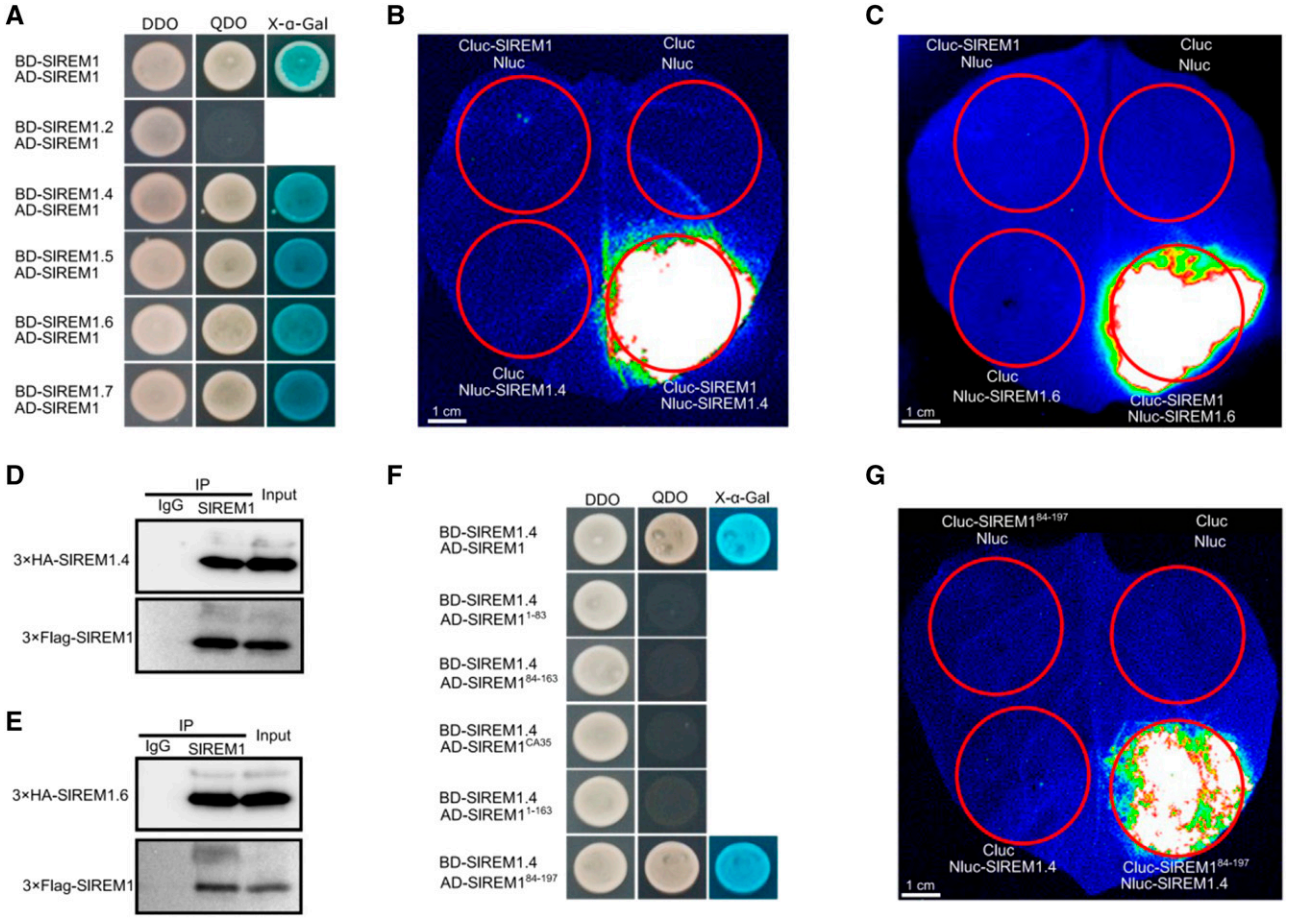

Figure 4. SlREM1 interacts with other members in remorin family. A, Y2H analysis for the interactions between SlREM1 and SlREM1, SlREM1.2, SlREM1.4, SlREM1.5, SlREM1., and SlREM1.7. DDO, SD/-Leu-Trp agar medium; QDO, SD/-Leu-Trp-His-Ade agar medium. B and C, Split LCI analysis for the interactions between SlREM1 and SlREM1.4/ SlREM1.6. Images were collected at 2 dpi. Red circles indicate the infiltration areas. D and E, Coimmunoprecipitation analysis of the interactions between SlREM1 and SlREM1.4/ SlREM1.6. Total protein extracts (input) was coimmunoprecipitated with anti-SlREM1 and IgG and the immunoprecipitated proteins were analyzed by immunoblotting using anti-HA antibody and anti-Flag antibody. F, Y2H analysis of the interaction between SlREM1$^{84\text{-}197}$ and SlREM1.4. DDO, SD/-Leu-Trp agar medium; QDO, SD/-Leu-Trp-His-Ade agar medium. G, Split LCI analysis of SlREM1$^{84–197}$ to SlREM1.4 interaction. Images were collected at 2 dpi. Red circles indicate the infiltration areas.

quantification (iTRAQ) was performed to investigate the global changes of proteins in *N. benthamiana* leaves overexpressing *3×Flag-SlREM1*. The experimental workflow of iTRAQ is presented in Figure 5A. Proteins from the *N. benthamiana* leaves expressing *3×Flag-SlREM1* and *3×Flag* at 1 and 3 dpi were isolated and submitted to iTRAQ proteomic analysis. A total of 5,511, 5,008, and 4,921 proteins were identified with a global false discovery rate (FDR) $< 1\%$ in three independent biological replicates. The cutoff was calculated using a population statistics method according to Gan et al. (2007) and used to determine significant differences in protein abundance. Finally, a total of 272 proteins exhibited substantial alterations in *N. benthamiana* leaves expressing *3×Flag-SlREM1* compared to those in *N. benthamiana* leaves expressing *3×Flag* at 1 or 3 dpi (Fig. 5B; Supplemental Table S2). Hierarchical clustering showed that the proteins were classified into two main clusters, representing those exhibiting higher or lower abundance in *N. benthamiana* leaves expressing *3×Flag-SlREM1* relative to those in the leaves expressing *3×Flag* (Fig. 5B). For proteins at 1 dpi, 11 and 35 proteins exhibited lower abundance and higher abundance, respectively. However, 145 and 120 proteins showed higher and lower abundance, respectively, at 3 dpi (Fig. 5C). When comparing the proteins showing variations in abundance between the leaves expressing *3×Flag-SlREM1* at 1 and 3 dpi, a total of 38 proteins overlapped (Fig. 5D; Supplemental Table S3). These results indicate that overexpression of *SlREM1* affects the protein expression profiles of *N. benthamiana* leaves.

According to the gene ontology annotations from agriGO2 (Tian et al., 2017), these differentially expressed proteins were classified into 16 functional categories (Supplemental Fig. S6). Among them, Response to stimulus, single-organism metabolic process,

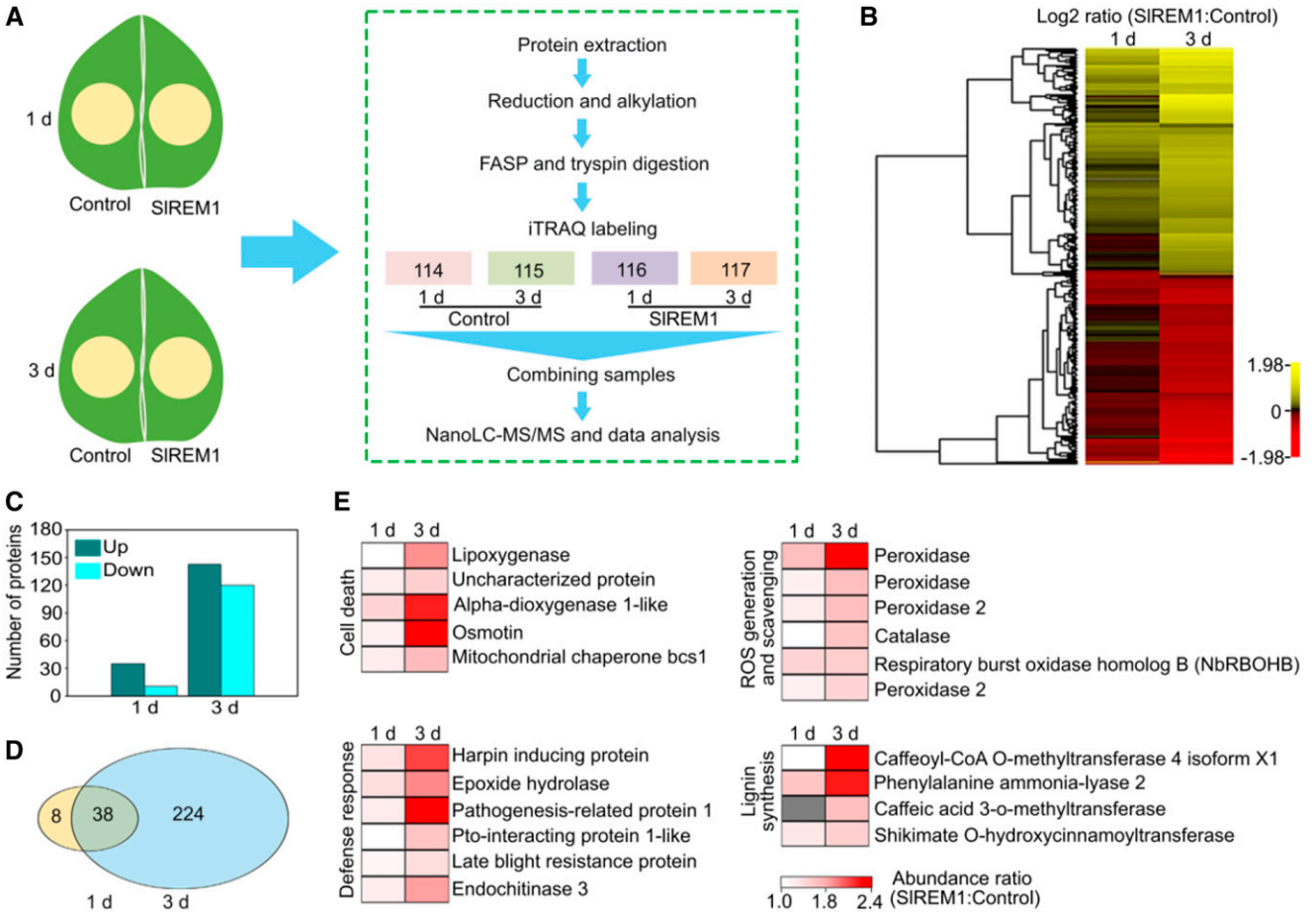

Figure 5. Quantitative proteomic analysis of *N. benthamiana* leaves transiently expressing *3×Flag-SlREM1*. A, The experimental workflow for quantitative proteome analysis. Total proteins were extracted from *N. benthamiana* leaves transiently expressing *3×Flag-SlREM1* (SlREM1) and *3×Flag* (control check [CK]) and subjected to iTRAQ analysis. The four different colors used oin the right representation different labeling reagents (115, 116, 117, and 118) used in the iTRAQ experiment. B, Total of 272 proteins showing differential expression were identified in *N. benthamiana* leaves transiently expressing *3×Flag-SlREM1* (SlREM1) compared to the CK. Proteins showing significant changes in abundance were hierarchically clustered based on the abundance ratio as a $\log_2$ scale. Each row in the color heat map represents a single protein. The yellow and red colors represent upregulated and down-regulated proteins, respectively, in the *N. benthamiana* leaves transiently expressing *3×Flag-SlREM1* relative to the control. Values represent the average of three biological replicates. The differentially regulated proteins are listed in Supplemental Table S2. C, The number of proteins showing higher or lower abundance in *N. benthamiana* leaves transiently expressing *3×Flag-SlREM1* relative to the control at 1 and 3 dpi. D, The overlapped proteins identified at 1 and 3 dpi in *N. benthamiana* leaves transiently expressing *3×Flag-SlREM1* relative to the control. E, Identification of proteins involved in cell death, ROS generation and scavenging, defense response, and lignin biosynthesis in quantitative proteome. Gray box indicates that the protein is not identified at 1 d. Abundance ratios were calculated using CK as denominator and plotted in a heat map. Values represent the average of three biological replicates.

oxidation-reduction process, and response to abiotic stimulus are the largest categories at 1 and 3 dpi. Notably, five proteins were allocated to the category of cell death (Fig. 5E), including lipoxygenase, uncharacterized protein, α-dioxygenase 1-like, osmotin, and mitochondrial chaperone bcs1, which are all putative orthologs of previously identified cell death regulators (De León et al., 2002; Hwang and Hwang, 2010; He et al., 2011; Choi et al., 2013a; Zhang et al., 2014a). Moreover, some defense response proteins, including harping inducing protein, epoxide hydrolase, basic form of pathogenesis-related protein1, Pto-interacting protein 1-like, Late blight resistance protein homology R1A-3 and endochitinase3, and lignin biosynthesis proteins displayed substantially increased abundance in the leaves expressing *3×Flag-SlREM1* (Fig. 5E). Strikingly, the abundance of NbRBOHB was also substantially upregulated in the leaves expressing *3×Flag-SlREM1*.

SlREM1 Stimulate ROS Production in *N. benthamiana* Leaves

ROS play a vital role in plant cell death (van Breusegem and Dat, 2006). RBOHs are plant NADPH oxidases, and are located on the PM to be critical for

ROS production (Kobayashi et al., 2006; Suzuki et al., 2011). *NbRBOHA* and *NbRBOHB* are two major producers for ROS burst in *N. benthamiana* leaves (Yoshioka et al., 2003). Our iTRAQ results showed that the abundance of NbRBOHB was substantially upregulated in the *N. benthamiana* leaves expressing *3×Flag-SlREM1* (Fig. 5E). To investigate whether the expression of *NbRBOHB* was enhanced by *SlREM1* overexpression, *GFP-SlREM1* and *GFP* were transiently expressed, followed by reverse transcription quantitative PCR (RT-qPCR) to assess the transcription of *NbRBOHB* in the leaves at 0, 1 and 3 dpi. As shown in Figure 6A, consistent with the changes in protein abundance, the transcript level of *NbRBOHB* was significantly increased at 1 and 3 dpi in the leaves overexpressing *GFP-SlREM1* compared to *GFP*, whereas no significant difference was observed for *NbRBOHA*, suggesting that the expression of *NbRBOHB* is strongly induced by SlREM1. In the meantime, the cytosolic level of ROS was investigated in *N. benthamiana* leaves. The level of hydrogen dioxide (H_2O_2) in *N. benthamiana* leaves expressing *GFP-SlREM1* was significantly higher, compared to that expressing *GFP* (Fig. 6B). Coincidentally, 3, 3′-diaminobenzidine (DAB) and nitro blue tetrazolium (NBT) staining showed that the stains in the *GFP-SlREM1* overexpressing leaves were much darker and increased dramatically over time compared to the control leaves (Fig. 6, C and D). This indicated that overexpression of *SlREM1* enhances ROS accumulation in *N. benthamiana* leaves, suggesting that SlREM1 can induce NbRBOHB expression and enhance ROS accumulation.

Identification of Previously Identified Regulators Involved in Cell Death

Based on iTRAQ, 38 proteins were upregulated in *N. benthamiana* leaves expressing *3×Flag-SlREM1* at 1 and 3 d, suggesting that these upregulated proteins may play important roles in SlREM1-induced cell death. Among them, 27 upregulated proteins have not been reported. To investigate whether these 27 proteins exhibited consistent patterns in transcript level and protein level, RT-qPCR was conducted to analyze transcript levels. As shown in Figure 7A, the transcript levels of 27 proteins substantially increased in *N. benthamiana* leaves expressing *3×Flag-SlREM1*, which were consistent with protein abundance in the iTRAQ. To reveal the role of these 27 proteins in SlREM1-induced cell death, they were transiently expressed in *N. benthamiana* leaves to evaluate the cell death phenotype. Three proteins, Cys-rich and transmembrane domain-containing protein A-like (CRTD), blue copper protein-like (BCPL), and nuclear cap-binding protein subunit2 (NCBP), were significantly upregulated in the leaves expressing *3×Flag-SlREM1* (Fig. 7B), and resulted in cell death in *N. benthamiana* leaves. Trypan blue

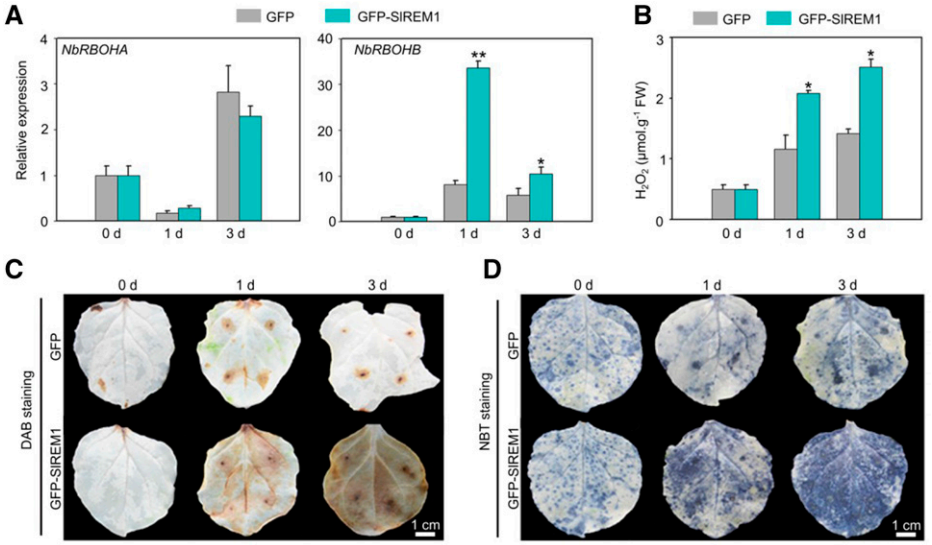

Figure 6. SlREM1 enhances ROS production in *N. benthamiana* leaves. A, Expression of *NbRBOHA* and *NbRBOHB* in the *N. benthamiana* leaves transiently expressing *GFP* and *GFP-SlREM1*. Total RNAs were isolated from *N. benthamiana* leaves transiently expressing *GFP-SlREM1* and *GFP* and further analyzed using RT-qPCR. *NbEF1a* was used as an internal control. Data are means and SD of three independent biological replicates. Asterisks indicate significant differences compared with leaves expressing *GFP* using ANOVA with a post hoc Tukey's Honestly Significant Difference test (*$P < 0.05$ and **$P < 0.01$). B, Accumulation of H_2O_2 in the *N. benthamiana* leaves transiently expressing *GFP* and *GFP-SlREM1*. Data are means and SD of three independent biological replicates. Asterisk indicates significant difference compared with leaves expressing GFP using ANOVA with a post hoc Tukey's Honestly Significant Difference test (*$P < 0.05$). C and D, DAB staining and NBT staining assays. *N. benthamiana* leaves transiently expressing *GFP-SlREM1* and *GFP* at 0, 1, and 3 dpi were subjected to ROS accumulation detection. The leaves were digitally extracted for comparison.

staining showed that the leaf areas expressing *CRTD*, *BCPL*, and *NCBP* were stained much darker compared to the control (Fig. 7C). Altogether, overexpression of *SlREM1* also promotes other cell death regulators to trigger cell death.

Phosphorylation Residues Interfere with SlREM1 Function

As remorin protein was first discovered as a phosphorylated protein in the presence of oligogalacturonides (Farmer et al., 1989), we presumed that SlREM1 could be phosphorylated, and phosphorylation may be important for SlREM1 function. To identify potential phosphorylation sites in SlREM1, GFP-SlREM1 and 3×HA-SlREM1 were transiently expressed in *N. benthamiana* leaves, immune-purified using anti-GFP and anti-HA antibodies beads, and then submitted for mass spectrometry (MS) identification. Finally, five phosphorylated residues were identified in the GFP- and HA-tagged SlREM1 protein. Ser at amino acid positions 52, 73, 90, and 120 as well as Thr at amino acid position 85 were phosphorylated and listed in Figure 8A and Supplemental Figure S7. To determine the role of the phosphorylated residues in SlREM1, phosphorylated residues were substituted by Ala or Asp to generate phosphorylation-deactivated $SlREM1^{5A}$ or activation $SlREM1^{5D}$. Subsequently, GFP-$SlREM1^{5A}$ and GFP-$SlREM1^{5D}$ were transiently expressed in *N. benthamiana* leaves. Immunoblot analysis with anti-GFP antibody showed that the GFP-SlREM1, GFP-$SlREM1^{5A}$, and GFP-$SlREM1^{5D}$ proteins were properly expressed in infiltrated *N. benthamiana* leaves (Supplemental Fig. S8). Trypan blue staining showed that leaf area expressing *GFP-$SlREM1^{5A}$* displayed

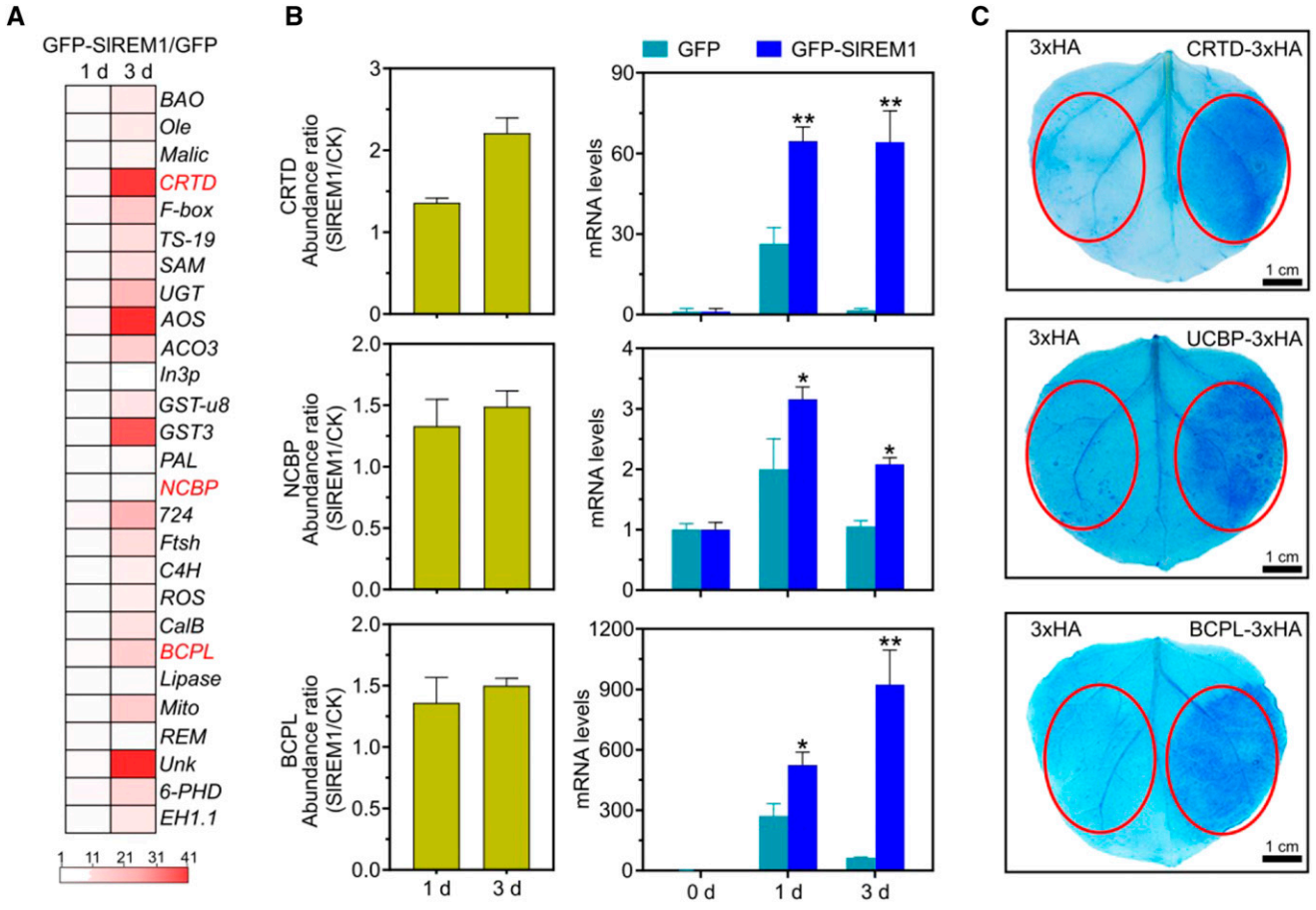

Figure 7. Identification of regulators involved in cell death. A, Changes in transcript levels of 27 upregulated proteins in *N. benthamiana* leaves transiently expressing *GFP* and *GFP-SlREM1*. Total RNA was isolated from the *N. benthamiana* leaves transiently expressing *GFP-SlREM1* and *GFP*, further analyzed by RT-qPCR and normalized relative to *NbEF1a* expression level. Each row in the color heat map represents a single gene. The white and red colors represent transcript levels showing changes in 1 to 41 folds in the *N. benthamiana* leaves transiently expressing *3×Flag-SlREM1* relative to the control. Values represent the ratio between GFP-SlREM1 and GFP. B, Comparison between protein abundance and mRNA level. The abundance of protein was assessed by iTRAQ analysis and mRNA levels were monitored by RT-qPCR. Asterisks indicate significant differences compared with leaves expressing GFP using ANOVA with a post hoc Tukey's Honestly Significant Difference test (*$P < 0.05$ and **$P < 0.01$).The values are presented as the means ± SD. C, *N. benthamiana* leaves transiently expressing *CRTD*, *BCPL*, and *NCBP* were stained with trypan blue at 5 dpi. Red circles indicate the infiltration areas.

much lighter blue than the area expressing *GFP-SlREM1*, whereas no difference was observed in the leaf area expressing *GFP-SlREM1^{5D}* and *GFP* (Fig. 8B), indicating that cell death induced by SlREM1^{5A} and SlREM1^{5D} was greatly reduced after substitution of phosphorylated residues. These results suggest that phosphorylation plays an important role in SlREM1-induced cell death.

In addition, the effects of phosphorylation on SlREM1 protein interaction and localization were also investigated. As shown in Figure 8C, the yeast cells cotransformed with SlREM1^{5A} and SlREM1 could grow and turn blue on SD/-Leu-Trp-His-Ade agar medium plus X-α-Gal, whereas the yeast cells cotransformed with SlREM1^{5D} and SlREM1 did not grow on SD/-Leu-Trp-His-Ade agar medium, indicating that SlREM1 can interact with SlREM1^{5A}, but not with SlREM1^{5D}. However, substitution of phosphorylated residues in SlREM1 protein did not influence the PM localization (Fig. 8D). Taken together, five phosphorylation residues interfere with SlREM1 function.

DISCUSSION

PCD is a genetically regulated phenomenon of cell self-elimination and displays a variety of functions in stress response (Lam, 2004). HR is a type of PCD that

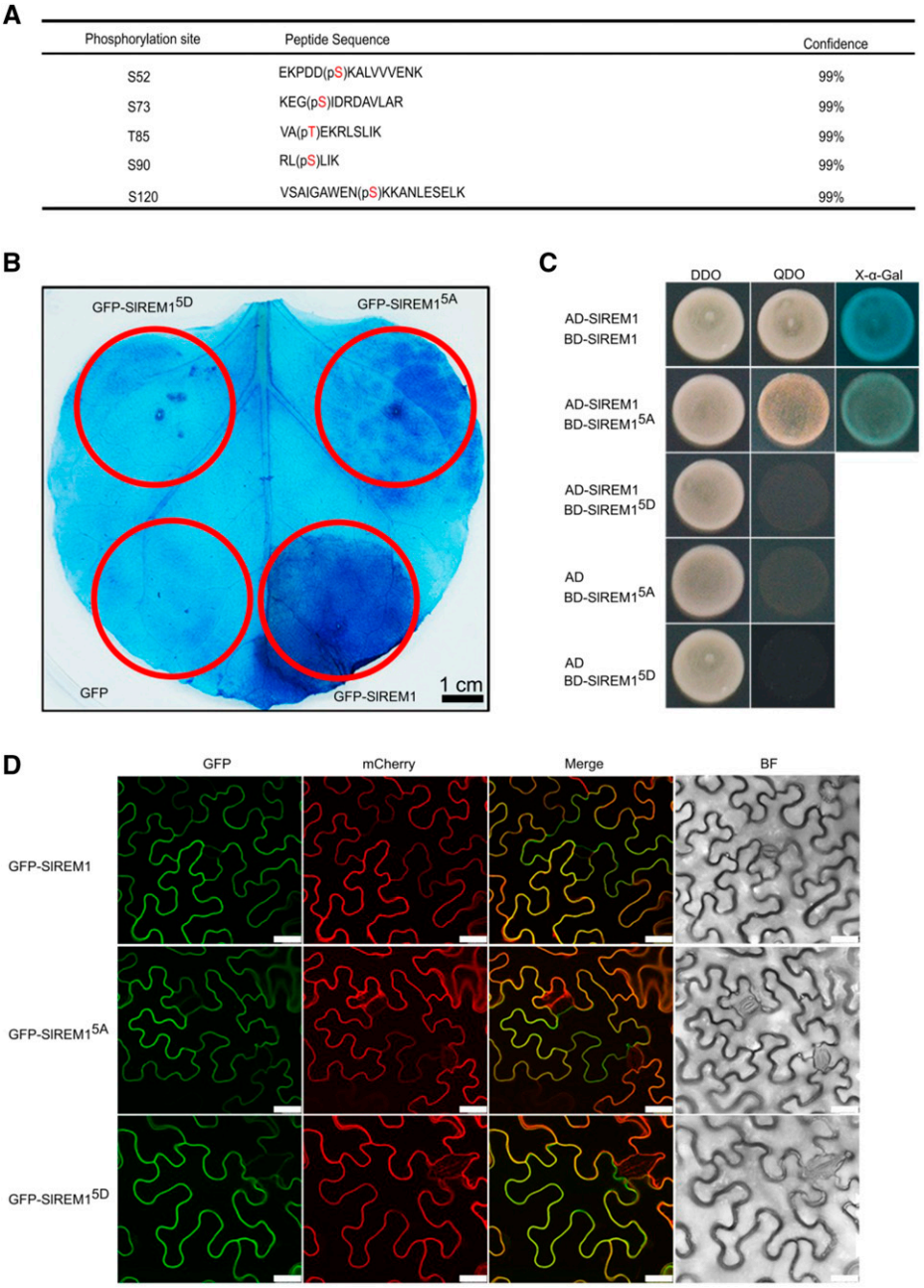

Figure 8. Five phosphorylation residues are essential for SlREM1-induced cell death. A, Five phosphorylation residues were identified in GFP-SlREM1 and 3×HA-SlREM1 proteins by MS. GFP-SlREM1 and 3×HA-SlREM1 were transiently expressed in *N. benthamiana* leaves, then purified using anti-GFP and HA beads, respectively, and further analyzed with MS. Red letters within brackets represent the phosphorylated residues. p, Phosphorylation. Phosphorylated peptides were accepted when their confidences calculated by the software ProteinPilot 5.0 were >99%. B, Mutation analysis for the five phosphorylation residues on SlREM1 cell death induction. SlREM1^{5A} and SlREM1^{5D} indicate that five phosphorylation residues were substituted by Ala or aspartic acids to generate phosphorylation deactivation SlREM1^{5A} or activation SlREM1^{5D}. Trypan blue staining was performed to evaluate the ability of cell death induction at 5 dpi. The red circles indicate the infiltration areas. C, Y2H analysis of the interactions among SlREM1 and SlREM1^{5A} and SlREM1^{5D}. DDO, SD/-Leu-Trp agar medium; QDO, SD/-Leu-Trp-His-Ade agar medium; X-α-Gal, 5-Bromo-4-chloro-3-indolyl-α-D-galactopyranoside. D, Mutations in the five phosphorylation residues did not change the localization of SlREM1. GFP-SlREM1, GFP-SlREM1^{5A}, and GFP-SlREM1^{5D} were transiently expressed in *N. benthamiana* leaves and the fluorescence was observed at 2 dpi. Scale bars = 25 μm.

occurs in response to pathogen attack, and is frequently associated with resistance to biotrophic and hemibiotrophic pathogens (Lamb and Dixon, 1997; Morel and Dangl, 1997; Greenberg and Yao, 2004). Emerging evidence suggests that HR is beneficial for necrotrophic pathogens invasion. The biomass of *B. cinerea* could be substantially inhibited in the HR-deficient mutant *dnd1* and dramatically increased by HR (Govrin and Levine, 2000). *B. cinerea* overexpressing a cell death inducer-BcXYG1 produced early local necrosis in leaves (Zhu et al., 2017). REM are plant-specific proteins and play important roles in biotic and abiotic stress response (Raffaele et al., 2009; Checker and Khurana, 2013). In this study, we found a previously unidentified function of *SlREM1* mediating plant cell death. Overexpression of *SlREM1* decreased the resistance of tomato leaves to necrotrophic pathogen *B. cinerea* (Fig. 1, A and B), and induced cell death in *N. benthamiana* leaves (Fig. 1, C, E, and F). Multiple SlREMs in subgroup I could interact with SlREM1 and also trigger cell death in *N. benthamiana* leaves (Figs. 3 and 4). These results demonstrate that *SlREM1* is a positive regulator of plant cell death for response to necrotrophic pathogen invasion.

Subcellular localization of a protein is important for its function. REM proteins localized in PM and contributed to plant defense response (Raffaele et al., 2009), grain setting in rice (Gui et al., 2014), and fruit ripening (Cai et al., 2018). Some studies demonstrated that C-terminal 28 amino acids of StREM1.3 and C-terminal 45 amino acids of GSD1 were required and sufficient for their PM localization (Perraki et al., 2012; Gui et al., 2015). Additionally, *S*-acylation of C-terminal Cys also play a vital role in remorin protein PM localization (Konrad et al., 2014; Fu et al., 2018). However, no putative *S*-acetylation site was predicted in SlREM1. Our results indicated that, among a series of deletion mutants, only SlREM1 containing C-terminal 35 amino acids could localize to PM, but deficiency, partial deficiency, or mutation of 35 amino acids caused SlREM1 to display cytoplasmic or nuclear localization (Fig. 2), suggesting that these C-terminal 35 amino acids are necessary for SlREM1 PM localization. Meanwhile, SlREM1 without the C-terminal 35 amino acids could not interact with SlREM1.4 (Fig. 4, F and G), indicating C-terminal 35 amino acids are required but not sufficient for the hetero- and homocomplex formation. Numerous critical domains involved in cell death induction were identified in the cell death regulator (Yu et al., 2012; Schreiber et al., 2016). Mutation of the P-loop motif abolishes RGA4-induced cell death and HR signaling activation (Césari et al., 2014). HD-Zip domain is vital for NbHB1 cell death induction (Yoon et al., 2009). Mutation of RXXS motif blocks ATL1-triggered cell death (Serrano et al., 2014). Our further studies showed that $SlREM1^{1–187}$ could also induce cell death, whereas $SlREM1^{1–187(15mu)}$, $SlREM1^{1–197(15mu)}$, and $SlREM1^{1–197(15del)}$ fail to trigger cell death (Fig. 2), indicating that amino acids 173 to 187 play a vital role in SlREM1 cell death induction.

Plant cell death is a genetically regulated process that is controlled by many regulators. Up to now, many cell death regulators, including MAPK cascade, transcription factors, proteases, and ROS and ROS generators, have been identified. However, the mechanisms are still not clear. In this study, an iTRAQ-based quantitative proteomic analysis showed that ~272 proteins displayed substantial changes in abundance during the process of SlREM1-induced cell death (Fig. 5, A and B; Supplemental Table S2). Some known cell death regulators, including lipoxygenase (Hwang and Hwang, 2010), uncharacterized protein (He et al., 2011), alpha-dioxygenase 1-like (García-Marcos et al., 2013), osmotin (Choi et al., 2013a), and mitochondrial chaperone bcs1 (Zhang et al., 2014a), were also identified in our study (Fig. 5E). Particularly, three upregulated proteins, CRTD, BCPL, and NCBP, were characterized as novel cell death positive regulators (Fig. 7, B and C), suggesting that they contribute to SlREM1 cell death induction. Cell death is closely associated with elevated levels of ROS. Exogenous H_2O_2 treatment could induce rapid cell death in soybean (*Glycine max*; Solomon et al., 1999) and *N. benthamiana* suspension cells (Houot et al., 2001). Application of ROS scavengers substantially inhibited or retarded cell death in Arabidopsis (Wrzaczek et al., 2009). Additionally, we found that the transcript and protein abundance of *NbRBOHB* significantly enhanced with increasing *SlREM1* expression (Fig. 6A). Simultaneously, the levels of H_2O_2 and O^{2-} were dramatically enhanced in *N. benthamiana* leaves expressing *SlREM1* (Fig. 6, B and C). These results demonstrated that overexpression of *SlREM1* could enhance the *NbRBOHB* expression and stimulate ROS bursts. Taken together, SlREM1 triggers cell death through activating the ROS burst and inducing other cell death regulators.

Phosphorylation serves as one of the most important post-translation modifications and plays an important role in regulating protein function (Pawson and Scott, 2005). Numerous researches have shown that phosphorylation is closely associated with a series of biological processes, including photomorphogenesis (Lin et al., 2017), leaf senescence (Ren et al., 2017), hormone signaling (Zhang et al., 2018), flowering (Su et al., 2017), seed germination (Yin et al., 2018), stomatal development (Yang et al., 2015), and immune response (Li et al., 2014). Similarly, striking evidence supported that phosphorylation was critical for PCD, and many kinases involved in PCD were isolated (Meng and Zhang, 2013). Remorin protein was originally discovered as a phosphorylated protein (Farmer et al., 1989). In this study, we identified five phosphorylation sites in SlREM1 protein (Fig. 8A), three of which are evolutionarily conserved positions of S73, T85, and S90 (Perraki et al., 2018). Further results showed phosphorylation substantially affected the ability of SlREM1 to trigger cell death and protein interaction (Fig. 8, B and C), but did not influence the localization of SlREM1 (Fig. 8D). These data indicate that phosphorylation contributes to the regulation of SlREM1 function.

Cell death serves as a proxy for effector-triggered immunity (ETI) caused by loss-of-function or gain-of-function of plant immune regulators (Pitsili et al., 2019). In some cases, pathogens deploy effectors to modify or degrade host proteins functioning as "guardees," whereas plant immune receptors with nucleotide-binding, Leu-rich repeat domains (NB-LRR, i.e. NLRs) can detect the modification and thus guard these "guardees", subsequently activating NLRs signaling and ETI (Césari, 2018). For instance, the cell death phenotype in *acd11* relied on the NLR LAZ5, and *acd11* was rescued by *laz5* knockout or dominant negative allele, indicating that ACD11 was probably an effector target guarded by LAZ5 (Palma et al., 2010). Similarly, RPM1-interacting protein4 was also guarded by multiple NLRs, such as RPM1 and RPS2, whereas interference with RPM1-interacting protein4 may activate these NLRs and further trigger ETI signaling (Rodriguez et al., 2016). Moreover, it was recently reported that NbREM4 interacted with and was phosphorylated by the immune receptor-like kinase PBS1 (which was cleaved by AvrPphB), and NbREM4 also directly interacted with the effector HopZ1a (Albers et al., 2019). Given that *SlREM1* overexpression dramatically upregulated late blight resistance protein homology R1A-3 and the observed cell death phenotype was also regulated by phosphorylation status of SlREM1, we were prompted to examine whether SlREM1 may be guarded by certain NLRs. As revealed by studies on autoimmune mutants and their respective NLR pairs, it may be necessary to interfere with several signaling components synergistically functioning in the complex. Alternatively, there may be some other undefined NLRs serving as the guard independent of the NLRs we have tested. More efforts may be made to ascertain this hypothesis in future work.

In conclusion, we find that *SlREM1* overexpression decreases the resistance of tomato leaves to *B. cinerea* and triggers cell death in *N. benthamiana* leaves, and prove that multiple SlREMs can form a complex to regulate cell death, then reveal that SlREM1 triggers cell death by activating ROS burst and other cell death regulators. Our data report the previously unknown function of SlREMs and provide insights for unraveling the molecular regulation networks of plant cell death.

MATERIALS AND METHODS

Plant Materials

Wild-type tomato (*Solanum lycopersicum* 'Ailsa Craig') and wild-type *Nicotiana benthamiana* were grown in controlled glasshouse conditions at 24°C with 60% relative humidity and 16-h light/8-h dark. The *SlREM1* transgenic plants (overexpression and RNA interference lines) used were as described in Cai et al. (2018).

Microbial Infection

Infection of tomato leaves by *Botrytis cinerea* was performed according to the methods of Zhang et al. (2016). *B. cinerea* strain B05.10 was cultured on potato dextrose agar medium at 23°C. Conidia of *B. cinerea* were resuspended in potato dextrose broth medium at a final concentration of 2×10^5 conidia per milliliter. Leaves were detached from 4- to 5-week–old tomato plants, inoculated with 5 μL of conidial suspension, and enclosed in plastic trays maintained at a high relative humidity (95%). Disease severity was evaluated every 12 h. Twenty-four leaves were collected from each transgenic line and used for microbial infection.The experiment was repeated twice.

Plasmid Construction for Transient Expression Experiments

The open reading frame (ORF) of *SlREM1*, truncations, and target genes were amplified with specific primers from complementary DNA (cDNA) of tomato and *N. benthamiana* leaves and cloned into pEAQ vector with 3×Flag, 3×HA, and GFP. The resulting plasmids were subsequently transferred into *Agrobacterium tumefaciens* strain GV3101. Utilized primers were listed in Supplemental Table S4.

Agrobacterium-Mediated Transient Expression in *N. benthamiana* Leaves

An *A. tumefaciens* GV3101 strain harboring the recombinant constructs was grown 1 d at 28°C in Luria-Bertani medium in the presence of kanamycin, gentamicin, and rifampicin, respectively. Afterward, the bacterial cells were harvested by centrifugation, resuspended in MM buffer (10 mM of MES at pH 5.7, 10 mM of $MgCl_2$, and 100 μM of acetosyringone) to $OD_{600} = 0.3$, and incubated for 2 h before infiltration. Four-week–old *N. benthamiana* leaves were infiltrated from the abaxial side using a 1-mL syringe without needle. At 2 dpi, leaves were collected to observe the green and red fluorescence under a TCS SP5 microscope (Leica). Cell death symptoms were evaluated and photographed at 6 dpi.

Electrolyte Leakage Assay

Electrolyte leakage assay was conducted according to the method of Mackey et al. (2002). *N. benthamiana* leaf discs (diameter 1.0 cm) were harvested from three infiltrated leaves, washed with deionized water for three times, and floated on 4 mL of deionized water for 3 h at 100 rpm at 25°C. The water conductivity was measured at the end of incubation with a conductivity meter (model no. SensION 7; Hach). This experiment was repeated three times.

Trypan Blue Staining

Trypan blue staining was performed according to the method described by Bai et al. (2012) with minor modifications. Briefly, six infiltrated leaves were harvested and immersed in lactophenol-trypan blue solution (2.5 mg mL^{-1} trypan blue, 25% [v/v] lactic acid, 25% [v/v] phenol, and 25% [v/v] glycerol) for 4 min at 95°C. The stained leaves were transferred to chloral hydrate buffer to remove chlorophyll. This experiment was repeated twice.

DAB Staining, NBT Staining, and Measurement of H_2O_2

DAB and NBT staining were performed according to the method of Jambunathan (2010). Briefly, six infiltrated leaves were detached, immersed in a DAB-staining buffer containing 1 mg mL^{-1} DAB-HCl at pH 3.8 (Sigma-Aldrich) and an NBT-staining buffer containing 1 mg mL^{-1} NBT at pH 3.8 (Sigma-Aldrich) in the dark for 8 h, respectively. After that, the leaves were destained by boiling in 70% (v/v) ethanol and photographed. These experiments were repeated three times.

The content of H_2O_2 was measured according to the method of Meng et al. (2014). Approximately 0.5 g of leaves expressing *3×Flag* and *3×Flag-SlREM1* were harvested, homogenized with 3 mL cold acetone, and then centrifuged at $2{,}000 \times g$ for 15 min. One milliliter of supernatant was collected and mixed with 100-μL 5% (w/v) titanium sulfate and 200-μL 25% (w/v) NH_4OH. The mixture was centrifuged at $10{,}000 \times g$ for 10 min and washed with acetone five times. The precipitate was dissolved in 5 mL of 2 M of H_2SO_4 and then acetone was added to 10 mL. The absorbance of the sample was determined at 410 nm. The experiment was repeated twice.

Phylogenetic Analysis

Amino acid sequences of Remorin proteins from tomato, *N. benthamiana*, rice (*Oryza sativa*), and Arabidopsis (*Arabidopsis thaliana*) were collected from Sol Genomics Network (https://solgenomics.net), Rice Genome Annotation Project (http://rice.plantbiology.msu.edu/analyses.shtml), and The Arabidopsis Information Resource (https://www.arabidopsis.org), respectively. All sequences are listed in Supplemental Table S5. Sequences were aligned using ClustalX (version 2.1; http://www.clustal.org/clustal2/) software with default multiple parameters and the point accepted mutation series protein weight. The alignment was imported into MEGA (version X; https://www.megasoftware.net/) software and the unrooted phylogenetic tree was constructed by the neighbor-joining method with 1,000 bootstrap replicates, using default parameters (Kumar et al., 2018).

Protein Extraction, iTRAQ Labeling, and Nano Liquid Chromatography Tandem MS Analysis

Proteins were extracted from *N. benthamiana* leaves transiently expressing *3×Flag-SlREM1* and *3×Flag* at 1 and 3 dpi according to the method described by Saravanan and Rose (2004). The isolated proteins were resuspended in the lysis buffer consisting of 500 mM of triethylammonium bicarbonate and 1% SDS (w/v) at pH 8.5 and sonicated at 35% amplitude for 3 min. After sonication, the supernatant was collected by centrifugation and the protein concentrations were quantified using a BCA Protein Assay Kit (Pierce). One-hundred micrograms of protein from each sample were reduced with Tris-(2-carboxyethyle) phosphine and alkylated with methylmethanethiosulfonate. After that, proteins were digested using trypsin following the filter-aided sample preparation method (Wiśniewski et al., 2009). The tryptic peptides were labeled using an iTRAQ Reagents 4-plex Kit (Applied Biosystems) according to the manufacturer's protocol. Peptides from the leaves transiently expressing *3×Flag* at 1 and 3 dpi were labeled with iTRAQ tags 114 and 115, whereas peptides from the leaves transiently expressing *3×Flag-SlREM1* at 1 and 3 dpi were labeled with iTRAQ tags 116 and 117, respectively. The labeled peptides were mixed, dried, and subjected to MS analysis. A Triple TOF 5600 Plus mass spectrometer (AB SCIEX) coupled with a NanoLC system (NanoLC–2D Ultra Plus; Eksigent) was used for MS analysis as described in Wang et al. (2014). Three independent biological replicates were performed in the iTRAQ experiment.

ProteinPilot 4.5 software (AB SCIEX) was used for protein identification and relative quantification of the iTRAQ experiments. *Nicotiana.proteins.fasta* (https://www.uniprot.org/) was set as the protein database for mass spectra data searching. The searching parameters were used as described in Wang et al. (2014). The Pro Group algorithm (AB SCIEX) was selected to evaluate the reporter peak area for iTRAQ quantification of peptide. The global FDR was calculated with a reverse database search strategy and used for peptide identification. Only proteins identified below 1% global FDR were quantified for the protein level. A population statistics was used to calculate the cutoff according the method proposed by Gan et al. (2007). The meaningful cutoff was used to verify the significance for the changes in abundance of all the identified proteins. Hierarchical clustering (Pearson algorithm) was performed with PermutMatrix software (Caraux and Pinloche, 2005).

Split LCI Assay

LCI assays were carried out according to the method proposed by Chen et al. (2008). The ORFs of *SlREM1*, *SlREM1.4*, and *SlREM1.6* were cloned into pCAMBIA1300-Cluc/Nluc to produce Cluc-SlREM1, SlREM1.4-Nluc, SlREM1.6-Nluc, and SlREM1-Nluc, respectively. Utilized primers were listed in Supplemental Table S6. The recombinant plasmids were transformed into *A. tumefaciens* strain GV3101 and infiltrated into *N. benthamiana* leaves. At 2 dpi, 1 mM of luciferin containing 1% (v/v) Triton X-100 was sprayed onto leaves, which were kept in the dark for 5 min, and then leaves were detached to observe the fluorescence. The LCI images were captured using a 5200 Multi (Tanon). The experiment was repeated two times.

Y2H Assay

For Y2H assay, the ORFs of *SlREM1*, *SlREM1.2*, *SlREM1.4*, *SlREM1.5*, *SlREM1.6*, and *SlREM1.7* were amplified and cloned into pGADT7 and pGBKT7 to generate AD-SlREM1, BD-SlREM1, BD-SlREM1.2, BD-SlREM1.4, BD-SlREM1.5, BD-SlREM1.6, and BD-SlREM1.7 vectors, respectively. The recombinant constructs were cotransformed into yeast AH109 strain and screened on DDO (SD/-Leu-Trp) and QDO agar medium (SD/-Leu-Trp-His-Ade) containing X-α-Gal. AD and BD, AD-SlREM1 and BD, and AD and BD-SlREM1, SlREM1.2, SlREM1.4, SlREM1.5, SlREM1.6, and SlREM1.7 were set as controls. Utilized primers were listed in Supplemental Table S7.

RT-qPCR Analysis

Total RNA were isolated from leaves transiently expressing *GFP* and *GFP-SlREM1* using Trizol, then treated with genome DNA Eraser and synthesized cDNA using the PrimeScript reagent kit (Takara). A StepOne Plus Real-Time PCR System (Applied Biosystems) with SYBR Premix Ex Taq (Tli RNaseH Plus; Takara) were used to quantify the expression of genes. *NbEF1α* were used as the reference gene for normalization. Values reported represent the average of three biological replicates. The primers were listed in Supplementary Supplemental Table S8.

Phosphosite Identification

Phosphosite identification was performed using a well-established protocol (Cai et al., 2018). *N. benthamiana* leaves transiently expressing GFP-SlREM1 and 3×HA-SlREM1 at 2 dpi were harvested, ground in liquid nitrogen, and lysed in immunoprecipitate buffer (50 mM of Tris-HCl at pH 7.5, 150 mM of NaCl, 1% [v/v] NP-40, 50 μM of MG132, 1 mM of phenylmethylsulfonyl fluoride, 1 × protease inhibitor cocktail [Roche], and 1 × phosphatase inhibitor mixture [Transgene]). The lysis solution was centrifuged at 14,000 × *g* at 4°C for 15 min. The supernatant was incubated with GFP-trap (Chromotek) and HA antibody-coated agarose (Abmart) for 4 h at 4°C, respectively. Finally, the proteins were eluted using 0.1 M of Gly-HCl (pH 2.5), reduced with 5 mM of dithiothreitol, alkylated with 10 mM of iodoacetamide, and then digested with trypsin (Promega). The tryptic peptides were identified by liquid chromatography tandem MS and phosphorylation sites were analyzed with the software ProteinPilot 5.02 (AB SCIEX).

Site-Directed Mutagenesis

For the site-directed mutagenesis of SlREM1^{5A} and SlREM1^{5D}, DNA fragments were amplified by fusion PCR using primers (Supplemental Table S9) harboring the mutations. The mutated SlREM1^{5A} and SlREM1^{5D} proteins were each cloned into a pEAQ-GFP vector using an in-fusion enzyme (Vazyme).

Accession Numbers

Sequence data of the tomato, Arabidopsis, *N. benthamiana*, and rice genes that were used in this article can be found in Supplemental Table S10.

Supplemental Data

The following materials are available.

Supplemental Figure S1. Expression of SlREM1 in leaves of wild-type and SlREM1 transgenic plants.

Supplemental Figure S2. Heterologous expression of *GFP-SlREM1*-induced cell death in tobacco leaves.

Supplemental Figure S3. Subcellular localization of SlREM1, SlREM1^{CA35}, and SlREM1$^{1–163}$.

Supplemental Figure S4. Trypan blue staining showed the critical domain of SlREM1 involved in cell death.

Supplemental Figure S5. Split LCI analysis of the SlREM1$^{84–163}$–SlREM1.4 interaction.

Supplemental Figure S6. Functional categories of the proteins that changed abundance in the leaves transiently expressing *3×Flag-SlREM1* and *3×Flag*.

Supplemental Figure S7. Spectra of five identified phosphorylated peptide by MS in the SlREM1 protein.

Supplemental Figure S8. Immunoblot analysis of transiently expressed GFP-SlREM1, GFP-SlREM1^{5A}, and GFP-SlREM1^{5D} in *N. benthamiana* leaves at 2 dpi.

Supplemental Table S1. Tomato remorin protein (SlREMs) information

Supplemental Table S2. Identification of proteins that changed in abundance at 1 dpi and 3 dpi in the leaves expressing *3×Flag-SlREM1* from iTRAQ-based quantitative proteomic analysis.

Supplemental Table S3. The overlapped proteins identified at 1 dpi and 3 dpi in leaves expressing *3×Flag-SlREM1* relative to leaves expressing *3×Flag*.

Supplemental Table S4. List of primers for plasmids construction.

Supplemental Table S5. List of Remorin protein sequences for phylogenetic tree construction.

Supplemental Table S6. Primers used in split LCI assays.

Supplemental Table S7. List of primers for Y2H assay.

Supplemental Table S8. Primers used in RT-qPCR.

Supplemental Table S9. List of primers for site-directed mutagenesis.

Supplemental Table S10. List of genes from tomato, Arabidopsis, *N. benthamiana*, and rice used in this study.

ACKNOWLEDGMENTS

The authors thank Dr. Zhuang Lu (Institute of Botany, Chinese Academy of Sciences) for analysis of tandem MS.

Received January 31, 2020; accepted March 23, 2020; published April 21, 2020.

LITERATURE CITED

Albers P, Üstün S, Witzel K, Kraner M, Börnke F (2019) A remorin from *Nicotiana benthamiana* interacts with the *Pseudomonas* type-III effector protein HopZ1a and is phosphorylated by the immune-related kinase PBS1. Mol Plant Microbe Interact **32:** 1229–1242

Bai S, Liu J, Chang C, Zhang L, Maekawa T, Wang Q, Xiao W, Liu Y, Chai J, Takken FLW, et al (2012) Structure-function analysis of barley NLR immune receptor MLA10 reveals its cell compartment specific activity in cell death and disease resistance. PLoS Pathog **8:** e1002752

Beers EP (1997) Programmed cell death during plant growth and development. Cell Death Differ **4:** 649–661

Beligni MV, Fath A, Bethke PC, Lamattina L, Jones RL (2002) Nitric oxide acts as an antioxidant and delays programmed cell death in barley aleurone layers. Plant Physiol **129:** 1642–1650

Bourque S, Dutartre A, Hammoudi V, Blanc S, Dahan J, Jeandroz S, Pichereaux C, Rossignol M, Wendehenne D (2011) Type-2 histone deacetylases as new regulators of elicitor-induced cell death in plants. New Phytol **192:** 127–139

Bozkurt TO, Richardson A, Dagdas YF, Mongrand S, Kamoun S, Raffaele S (2014) The plant membrane-associated REMORIN1.3 accumulates in discrete perihaustorial domains and enhances susceptibility to *Phytophthora infestans*. Plant Physiol **165:** 1005–1018

Cai J, Qin G, Chen T, Tian S (2018) The mode of action of remorin1 in regulating fruit ripening at transcriptional and post-transcriptional levels. New Phytol **219:** 1406–1420

Caraux G, Pinloche S (2005) PermutMatrix: A graphical environment to arrange gene expression profiles in optimal linear order. Bioinformatics **21:** 1280–1281

Césari S (2018) Multiple strategies for pathogen perception by plant immune receptors. New Phytol **219:** 17–24

Césari S, Kanzaki H, Fujiwara T, Bernoux M, Chalvon V, Kawano Y, Shimamoto K, Dodds P, Terauchi R, Kroj T (2014) The NB-LRR proteins RGA4 and RGA5 interact functionally and physically to confer disease resistance. EMBO J **33:** 1941–1959

Checker VG, Khurana P (2013) Molecular and functional characterization of mulberry EST encoding remorin (*MiREM*) involved in abiotic stress. Plant Cell Rep **32:** 1729–1741

Chen H, Zou Y, Shang Y, Lin H, Wang Y, Cai R, Tang X, Zhou JM (2008) Firefly luciferase complementation imaging assay for protein-protein interactions in plants. Plant Physiol **146:** 368–376

Choi DS, Hwang BK (2011) Proteomics and functional analyses of pepper abscisic acid-responsive 1 (ABR1), which is involved in cell death and defense signaling. Plant Cell **23:** 823–842

Choi HW, Kim NH, Lee YK, Hwang BK (2013b) The pepper extracellular xyloglucan-specific endo-β-1,4-glucanase inhibitor protein gene, *CaX-EGIP1*, is required for plant cell death and defense responses. Plant Physiol **161:** 384–396

Choi S, Hong JK, Hwang BK (2013a) Pepper osmotin-like protein 1 (CaOSM1) is an essential component for defense response, cell death, and oxidative burst in plants. Planta **238:** 1113–1124

Coll NS, Epple P, Dangl JL (2011) Programmed cell death in the plant immune system. Cell Death Differ **18:** 1247–1256

De León IP, Sanz A, Hamberg M, Castresana C (2002) Involvement of the Arabidopsis α-DOX1 fatty acid dioxygenase in protection against oxidative stress and cell death. Plant J **29:** 61–62

Fan J, Bai P, Ning Y, Wang J, Shi X, Xiong Y, Zhang K, He F, Zhang C, Wang R, et al (2018) The monocot-specific receptor-like kinase SDS2 controls cell death and immunity in rice. Cell Host Microbe **23:** 498–510.e5

Farmer EE, Pearce G, Ryan CA (1989) In vitro phosphorylation of plant plasma membrane proteins in response to the proteinase inhibitor inducing factor. Proc Natl Acad Sci USA **86:** 1539–1542

Fu S, Xu Y, Li C, Li Y, Wu J, Zhou X (2018) *Rice stripe virus* interferes with S-acylation of remorin and induces its autophagic degradation to facilitate virus infection. Mol Plant **11:** 269–287

Fuchs Y, Steller H (2011) Programmed cell death in animal development and disease. Cell **147:** 742–758

Gan CS, Chong PK, Pham TK, Wright PC (2007) Technical, experimental, and biological variations in isobaric tags for relative and absolute quantitation (iTRAQ). J Proteome Res **6:** 821–827

García-Marcos A, Pacheco R, Manzano A, Aguilar E, Tenllado F (2013) Oxylipin biosynthesis genes positively regulate programmed cell death during compatible infections by the synergistic pair Potato virus X-Potato virus Y and by Tomato spotted wilt virus. J Virol **87:** 5769–5783

Gechev TS, van Breusegem F, Stone JM, Denev I, Laloi C (2006) Reactive oxygen species as signals that modulate plant stress responses and programmed cell death. BioEssays **28:** 1091–1101

Govrin EM, Levine A (2000) The hypersensitive response facilitates plant infection by the necrotrophic pathogen *Botrytis cinerea*. Curr Biol **10:** 751–757

Greenberg JT, Yao N (2004) The role and regulation of programmed cell death in plant-pathogen interactions. Cell Microbiol **6:** 201–211

Gui J, Liu C, Shen J, Li L (2014) *Grain setting defect1*, encoding a remorin protein, affects the grain setting in rice through regulating plasmodesmatal conductance. Plant Physiol **166:** 1463–1478

Gui J, Zheng S, Liu C, Shen J, Li J, Li L (2016) OsREM4.1 interacts with OsSERK1 to coordinate the interlinking between abscisic acid and brassinosteroid signaling in rice. Dev Cell **38:** 201–213

Gui J, Zheng S, Shen J, Li L (2015) Grain setting defect1 (GSD1) function in rice depends on S-acylation and interacts with actin 1 (OsACT1) at its C-terminal. Front Plant Sci **6:** 804

He S, Tan G, Liu Q, Huang K, Ren J, Zhang X, Yu X, Huang P, An C (2011) The LSD1-interacting protein GILP is a LITAF domain protein that negatively regulates hypersensitive cell death in Arabidopsis. PLoS One **6:** e18750

Houot V, Etienne P, Petitot AS, Barbier S, Blein JP, Suty L (2001) Hydrogen peroxide induces programmed cell death features in cultured tobacco BY-2 cells, in a dose-dependent manner. J Exp Bot **52:** 1721–1730

Huysmans M, Lema A S, Coll NS, Nowack MK (2017) Dying two deaths—programmed cell death regulation in development and disease. Curr Opin Plant Biol **35:** 37–44

Hwang IS, Choi DS, Kim NH, Kim DS, Hwang BK (2014a) Pathogenesis-related protein 4b interacts with leucine-rich repeat protein 1 to suppress PR4b-triggered cell death and defense response in pepper. Plant J **77:** 521–533

Hwang IS, Choi DS, Kim NH, Kim DS, Hwang BK (2014b) The pepper cysteine/histidine-rich DC1 domain protein CaDC1 binds both RNA and DNA and is required for plant cell death and defense response. New Phytol **201:** 518–530

Hwang IS, Hwang BK (2010) The pepper 9-lipoxygenase gene CaLOX1 functions in defense and cell death responses to microbial pathogens. Plant Physiol **152:** 948–967

Jambunathan N (2010) Determination and detection of reactive oxygen species ROS, lipid peroxidation, and electrolyte leakage in plants. Methods Mol Biol **639:** 291–297

Kaneda T, Taga Y, Takai R, Iwano M, Matsui H, Takayama S, Isogai A, Che FS (2009) The transcription factor OsNAC4 is a key positive regulator of plant hypersensitive cell death. EMBO J **28:** 926–936

Kobayashi M, Kawakita K, Maeshima M, Doke N, Yoshioka H (2006) Subcellular localization of StRBOH proteins and NADPH-dependent $O2^-$-generating activity in potato tuber tissues. J Exp Bot **57:** 1373–1379

Konrad SS, Popp C, Stratil TF, Jarsch IK, Thallmair V, Folgmann J, Marín M, Ott T (2014) S-acylation anchors remorin proteins to the plasma membrane but does not primarily determine their localization in membrane microdomains. New Phytol **203:** 758–769

Kumar S, Stecher G, Li M, Knyaz C, Tamura K (2018) MEGA X: Molecular evolutionary genetics analysis across computing platforms. Mol Biol Evol **35:** 1547–1549

Lam E (2004) Controlled cell death, plant survival and development. Nat Rev Mol Cell Biol **5:** 305–315

Lam E, Kato N, Lawton M (2001) Programmed cell death, mitochondria and the plant hypersensitive response. Nature **411:** 848–853

Lamb C, Dixon RA (1997) The oxidative burst in plant disease resistance. Annu Rev Plant Physiol Plant Mol Biol **48:** 251–275

Lee DH, Kim DS, Hwang BK (2012) The pepper RNA-binding protein CaRBP1 functions in hypersensitive cell death and defense signaling in the cytoplasm. Plant J **72:** 235–248

Lefebvre B, Timmers T, Mbengue M, Moreau S, Hervé C, Tóth K, Bittencourt-Silvestre J, Klaus D, Deslandes L, Godiard L, et al (2010) A remorin protein interacts with symbiotic receptors and regulates bacterial infection. Proc Natl Acad Sci USA **107:** 2343–2348

Li H, Chen Y, Zhang ZQ, Li BQ, Qin GZ, Tian SP (2018) Pathogenic mechanisms and control strategies of *Botrytis cinerea* causing postharvest decay in fruits and vegetables. Food Quality and Safety **3:** 111–119

Li L, Li M, Yu L, Zhou Z, Liang X, Liu Z, Cai G, Gao L, Zhang X, Wang Y, et al (2014) The FLS2-associated kinase BIK1 directly phosphorylates the NADPH oxidase RbohD to control plant immunity. Cell Host Microbe **15:** 329–338

Lin F, Xu D, Jiang Y, Chen H, Fan L, Holm M, Deng XW (2017) Phosphorylation and negative regulation of CONSTITUTIVELY PHOTOMORPHOGENIC 1 by PINOID in Arabidopsis. Proc Natl Acad Sci USA **114:** 6617–6622

Liu JZ, Whitham SA (2013) Overexpression of a soybean nuclear localized type-III DnaJ domain-containing *HSP40* reveals its roles in cell death and disease resistance. Plant J **74:** 110–121

Mackey D, Holt BF III, Wiig A, Dangl JL (2002) RIN4 interacts with *Pseudomonas syringae* type III effector molecules and is required for RPM1-mediated resistance in Arabidopsis. Cell **108:** 743–754

Meng X, Yin B, Feng HL, Zhang XQ, Liang Q, Meng QW (2014) Overexpression of *R2R3-MYB* gene leads to accumulation of anthocyanin and enhanced resistance to chilling and oxidative stress. Biol Plant **58:** 121–130

Meng X, Zhang S (2013) MAPK cascades in plant disease resistance signaling. Annu Rev Phytopathol **51:** 245–266

Morel JB, Dangl JL (1997) The hypersensitive response and the induction of cell death in plants. Cell Death Differ **4:** 671–683

Palma K, Thorgrimsen S, Malinovsky FG, Fiil BK, Nielsen HB, Brodersen P, Hofius D, Petersen M, Mundy J (2010) Autoimmunity in Arabidopsis *acd11* is mediated by epigenetic regulation of an immune receptor. PLoS Pathog **6:** e1001137

Pawson T, Scott JD (2005) Protein phosphorylation in signaling—50 years and counting. Trends Biochem Sci **30:** 286–290

Perraki A, Cacas JL, Crowet JM, Lins L, Castroviejo M, German-Retana S, Mongrand S, Raffaele S (2012) Plasma membrane localization of *Solanum tuberosum* remorin from group 1, homolog 3 is mediated by conformational changes in a novel C-terminal anchor and required for the restriction of *potato virus X* movement. Plant Physiol **160:** 624–637

Perraki A, Gronnier J, Gouguet P, Boudsocq M, Deroubaix AF, Simon V, German-Retana S, Legrand A, Habenstein B, Zipfel C, et al (2018) REM1.3's phospho-status defines its plasma membrane nanodomain organization and activity in restricting PVX cell-to-cell movement. PLoS Pathog **14:** e1007378

Phan HA, Iacuone S, Li SF, Parish RW (2011) The MYB80 transcription factor is required for pollen development and the regulation of tapetal programmed cell death in *Arabidopsis thaliana*. Plant Cell **23:** 2209–2224

Pitsili E, Phukan UJ, Coll NS (2019) Cell death in plant immunity. Cold Spring Harb Perspect Biol doi:10.1101/cshperspect.a036483

Qin G, Meng X, Wang Q, Tian S (2009) Oxidative damage of mitochondrial proteins contributes to fruit senescence: A redox proteomics analysis. J Proteome Res **8:** 2449–2462

Qu GQ, Liu X, Zhang YL, Yao D, Ma QM, Yang MY, Zhu WH, Yu S, Luo YB (2009) Evidence for programmed cell death and activation of specific caspase-like enzymes in the tomato fruit heat stress response. Planta **229:** 1269–1279

Raffaele S, Bayer E, Lafarge D, Cluzet S, German Retana S, Boubekeur T, Leborgne-Castel N, Carde JP, Lherminier J, Noirot E, et al (2009) Remorin, a *Solanaceae* protein resident in membrane rafts and plasmodesmata, impairs *Potato virus X* movement. Plant Cell **21:** 1541–1555

Raffaele S, Mongrand S, Gamas P, Niebel A, Ott T (2007) Genome-wide annotation of remorins, a plant-specific protein family: Evolutionary and functional perspectives. Plant Physiol **145:** 593–600

Ren Y, Li Y, Jiang Y, Wu B, Miao Y (2017) Phosphorylation of WHIRLY1 by CIPK14 shifts its localization and dual functions in Arabidopsis. Mol Plant **10:** 749–763

Rodriguez E, El Ghoul H, Mundy J, Petersen M (2016) Making sense of plant autoimmunity and 'negative regulators'. FEBS J **283:** 1385–1391

Saravanan RS, Rose JK (2004) A critical evaluation of sample extraction techniques for enhanced proteomic analysis of recalcitrant plant tissues. Proteomics **4:** 2522–2532

Schreiber KJ, Bentham A, Williams SJ, Kobe B, Staskawicz BJ (2016) Multiple domain associations within the Arabidopsis immune receptor RPP1 regulate the activation of programmed cell death. PLoS Pathog **12:** e1005769

Serrano I, Gu Y, Qi D, Dubiella U, Innes RW (2014) The Arabidopsis EDR1 protein kinase negatively regulates the ATL1 E3 ubiquitin ligase to suppress cell death. Plant Cell **26:** 4532–4546

Solomon M, Belenghi B, Delledonne M, Menachem E, Levine A (1999) The involvement of cysteine proteases and protease inhibitor genes in the regulation of programmed cell death in plants. Plant Cell **11:** 431–444

Su Y, Wang S, Zhang F, Zheng H, Liu Y, Huang T, Ding Y (2017) Phosphorylation of histone H2A at serine 95: A plant-specific mark involved in flowering time regulation and H2A. Z deposition. Plant Cell **29:** 2197–2213

Suzuki N, Miller G, Morales J, Shulaev V, Torres MA, Mittler R (2011) Respiratory burst oxidases: The engines of ROS signaling. Curr Opin Plant Biol **14:** 691–699

Tian S, Qin G, Li B (2013) Reactive oxygen species involved in regulating fruit senescence and fungal pathogenicity. Plant Mol Biol **82:** 593–602

Tian T, Liu Y, Yan H, You Q, Yi X, Du Z, Xu W, Su Z (2017) agriGO v2.0: A GO analysis toolkit for the agricultural community, 2017 update. Nucleic Acids Res **45**(W1): W122–W129

Urquhart W, Gunawardena AH, Moeder W, Ali R, Berkowitz GA, Yoshioka K (2007) The chimeric cyclic nucleotide-gated ion channel ATCNGC11/12 constitutively induces programmed cell death in a Ca^{2+} dependent manner. Plant Mol Biol **65:** 747–761

van Breusegem F, Dat JF (2006) Reactive oxygen species in plant cell death. Plant Physiol **141:** 384–390

Wang Y, Wang W, Cai J, Zhang Y, Qin G, Tian S (2014) Tomato nuclear proteome reveals the involvement of specific E2 ubiquitin-conjugating enzymes in fruit ripening. Genome Biol **15:** 548

Wiśniewski JR, Zougman A, Nagaraj N, Mann M (2009) Universal sample preparation method for proteome analysis. Nat Methods **6:** 359–362

Wrzaczek M, Brosché M, Kollist H, Kangasjärvi J (2009) Arabidopsis GRI is involved in the regulation of cell death induced by extracellular ROS. Proc Natl Acad Sci USA **106:** 5412–5417

Wu J, Sun Y, Zhao Y, Zhang J, Luo L, Li M, Wang J, Yu H, Liu G, Yang L, et al (2015) Deficient plastidic fatty acid synthesis triggers cell death by modulating mitochondrial reactive oxygen species. Cell Res **25:** 621–633

Xie HT, Wan ZY, Li S, Zhang Y (2014) Spatiotemporal production of reactive oxygen species by NADPH oxidase is critical for tapetal programmed cell death and pollen development in Arabidopsis. Plant Cell **26:** 2007–2023

Yang KZ, Jiang M, Wang M, Xue S, Zhu LL, Wang HZ, Zou JJ, Lee EK, Sack F, Le J (2015) Phosphorylation of serine 186 of bHLH transcription factor SPEECHLESS promotes stomatal development in Arabidopsis. Mol Plant **8:** 783–795

Yen CH, Yang CH (1998) Evidence for programmed cell death during leaf senescence in plants. Plant Cell Physiol **39:** 922–927

Yin X, Wang X, Komatsu S (2018) Phosphoproteomics: Protein phosphorylation in regulation of seed germination and plant growth. Curr Protein Pept Sci **19:** 401–412

Yoon J, Chung WI, Choi D (2009) NbHB1, *Nicotiana benthamiana* homeobox 1, is a jasmonic acid-dependent positive regulator of pathogen-induced plant cell death. New Phytol **184:** 71–84

Yoshie Y, Goto K, Takai R, Iwano M, Takayama S, Isogai A, Che FS (2005) Function of the rice gp91phox homologs *OsrbohA* and *OsrbohE* genes in ROS-dependent plant immune responses. Plant Biotechnol J **22:** 127–135

Yoshioka H, Numata N, Nakajima K, Katou S, Kawakita K, Rowland O, Jones JD, Doke N (2003) *Nicotiana benthamiana* gp91phox homologs NbrbohA and NbrbohB participate in H_2O_2 accumulation and resistance to *Phytophthora infestans*. Plant Cell **15:** 706–718

You Q, Zhai K, Yang D, Yang W, Wu J, Liu J, Pan W, Wang J, Zhu X, Jian Y, et al (2016) An E3 ubiquitin ligase-BAG protein module controls plant innate immunity and broad-spectrum disease resistance. Cell Host Microbe **20:** 758–769

Yu X, Tang J, Wang Q, Ye W, Tao K, Duan S, Lu C, Yang X, Dong S, Zheng X, et al (2012) The RxLR effector Avh241 from *Phytophthora sojae* requires plasma membrane localization to induce plant cell death. New Phytol **196:** 247–260

Zamyatnin AA Jr. (2015) Plant proteases involved in regulated cell death. Biochemistry (Mosc) **80:** 1701–1715

Zhang B, Van Aken O, Thatcher L, De Clercq I, Duncan O, Law SR, Murcha MW, van der Merwe M, Seifi HS, Carrie C, et al (2014a) The mitochondrial outer membrane AAA ATPase AtOM66 affects cell death and pathogen resistance in *Arabidopsis thaliana*. Plant J **80:** 709–727

Zhang L, Li X, Li D, Sun Y, Li Y, Luo Q, Liu Z, Wang J, Li X, Zhang H, et al (2018) CARK1 mediates ABA signaling by phosphorylation of ABA receptors. Cell Discov **4:** 30

Zhang Z, Li H, Qin G, He C, Li B, Tian S (2016) The MADS-Box transcription factor *Bcmads1* is required for growth, sclerotia production and pathogenicity of *Botrytis cinerea*. Sci Rep **6:** 33901

Zhang Z, Qin G, Li B, Tian S (2014b) Knocking out *Bcsas1* in *Botrytis cinerea* impacts growth, development, and secretion of extracellular proteins, which decreases virulence. Mol Plant Microbe Interact **27:** 590–600

Zhu W, Ronen M, Gur Y, Minz-Dub A, Masrati G, Ben-Tal N, Savidor A, Sharon I, Eizner E, Valerius O, et al (2017) BcXYG1, a secreted xyloglucanase from *Botrytis cinerea*, triggers both cell death and plant immune responses. Plant Physiol **175:** 438–456